Heliyon 6 (2020) e05263

Contents lists available at ScienceDirect

Heliyon

journal homepage: www.cell.com/heliyon

Research article

Microalgal metabolites as anti-cancer/anti-oxidant agents reduce cytotoxicity of elevated silver nanoparticle levels against non-cancerous vero cells

Hanaa Ali Hussein [a,b], M. Maulidiani [c], Mohd Azmuddin Abdullah [a,*]

[a] Institute of Marine Biotechnology, Universiti Malaysia Terengganu, 21030, Kuala Nerus, Terengganu, Malaysia
[b] College of Dentistry, University of Basrah, Basrah, Iraq
[c] Faculty of Science and Marine Environment, Universiti Malaysia Terengganu, 21030, Kuala Nerus, Terengganu, Malaysia

ARTICLE INFO

Keywords:
Environmental science
Toxicology
Cell biology
Biochemistry
Heavy metals
Microalgal metabolites
Silver nanoparticles
Apoptosis
Cell-cycle
Metabolite profiling

ABSTRACT

Heavy metal pollution has become a major concern globally as it contaminates eco-system, water networks and as finely suspended particles in air. In this study, the effects of elevated silver nanoparticle (AgNPs) levels as a model system of heavy metals, in the presence of microalgal crude extracts (MCEs) at different ratios, were evaluated against the non-cancerous Vero cells, and the cancerous MCF-7 and 4T1 cells. The MCEs were developed from water (W) and ethanol (ETH) as green solvents. The AgNPs-MCEs-W at the 4:1 and 5:1 ratios (v/v) after 48 and 72 h treatment, respectively, showed the IC_{50} values of 83.17–95.49 and 70.79–91.20 μg/ml on Vero cells, 13.18–28.18 and 12.58–25.7 μg/ml on MCF-7; and 16.21–33.88 and 14.79–26.91 μg/ml on 4T1 cells. In comparison, the AgNPs-MCEs-ETH formulation achieved the IC_{50} values of 56.23–89.12 and 63.09–91.2 μg/ml on Vero cells, 10.47–19.95 and 13.48–26.61 μg/ml on MCF-7; 14.12–50.11 and 15.13–58.88 μg/ml on 4T1 cells, respectively. After 48 and 72 h treatment, the AgNPs-MCE-CHL at the 4:1 and 5:1 ratios exhibited the IC_{50} of 51.28–75.85 and 48.97–69.18 μg/ml on Vero cells, and higher cytotoxicity at 10.47–16.98 and 6.19–14.45 μg/ml against MCF-7 cells, and 15.84–31.62 and 12.58–24.54 μg/ml on 4T1 cells, respectively. The AgNPs-MCEs-W and ETH resulted in low apoptotic events in the Vero cells after 24 h, but very high early and late apoptotic events in the cancerous cells. The Liquid Chromatography-Mass Spectrometry-Electrospray Ionization (LC-MS-ESI) metabolite profiling of the MCEs exhibited 64 metabolites in negative ion and 56 metabolites in positive ion mode, belonging to different classes. The microalgal metabolites, principally the anti-oxidative components, could have reduced the toxicity of the AgNPs against Vero cells, whilst retaining the cytotoxicity against the cancerous cells.

1. Introduction

Heavy metals are elements occurring naturally, and have high atomic weight and a density of at least 5 times the density of water. The presence and wide distribution of heavy metals in the environment are attributed to the anthropogenic activities such as mining and electro-plating industries, and also from agricultural and electronic wastes. There have been major concern on the potential effects of heavy metal pollution on the environment and human health that constant monitoring has become an essential part of the integrated remediation strategies [1, 2]. The toxicity of heavy metals depends on dosage, exposure route and duration, and chemical types. Exposure and impacts on individuals vary based on gender, age, genetics, and nutritional uptake. Heavy metals such as cadmium, arsenic, chromium, mercury, and lead, have high degree of toxicity, and are known to cause damage to many organs, even at low levels. These are among the priority metals of public health concern and classified as human carcinogens according to the International Agency for Research on Cancer and the U.S. Environmental Protection Agency [3].

Toxic level of heavy metals in drinking water and marine organisms such as fish, and in the food chains from unsustainable agricultural practices, and also released from vehicles and fumes could be among the factors that contribute towards the spike in cancer incidence globally. Breast cancer is the most prevalent cancer in women and early stage diagnosis to identify cancerous cells could decrease the mortality rates in the long term. The screening methods include mammography,

* Corresponding author.
E-mail addresses: azmuddin@umt.edu.my, joule1602@gmail.com (M.A. Abdullah).

https://doi.org/10.1016/j.heliyon.2020.e05263
Received 3 July 2020; Received in revised form 6 September 2020; Accepted 12 October 2020

ultrasound, magnetic resonance imaging, computerized tomography, biopsy and positron emission tomography [4]. New methods which are rapid and cost-effective have been developed as a promising diagnostic tool using sensors with biomarkers and intensive imaging techniques [4]. AgNPs are the type of metals, purportedly "safer", as characterized by their electrical, optical, and thermal properties, which can be integrated into the products ranging from optical to biological systems and chemical sensors. The pastes, conductive inks and fillers containing AgNPs have been incorporated to attain higher stability, electrical conductivity, and low sintering temperatures [5]. In biological and biomedical applications, the AgNPs exhibit antibacterial, antifungal, antiviral, anti-inflammatory, anti-cancer, and anti-angiogenic activities [6, 7, 8]. There are vast potentials for theranostic applications of the AgNPs, with the capacity for passive or active targeting of certain diseased cells or tumor tissues through the encapsulation or entrapment of the bioactive molecules. These are attractive features for applications in cancer diagnosis and bio-sensing [9], and as drug delivery vehicles and therapeutic agents [10].

Natural compounds could become the major source of novel therapeutic strategies against cancer [11]. Many marine natural compounds play essential roles in drug development, either directly as drugs or as key molecules for the synthesis of biochemical drugs [12, 13]. Compounds such as didemnin B, dolastatin 10, girolline, bengamide derivative, cryptophycins, bryostatin 1 and kahalalide F, have already been used in clinical trials for cancer, allergy, analgesia, and cognitive diseases [14]. Microalgae have the potential to improve health and minimize the risk of disease development. There has been an emergence of microalgal natural products with potent antitumoral and anti-infectious activities [15]. The varied habitat of microalgae leads to diverse biologically active compounds, which are either primary or secondary metabolites, that can be obtained from the biomass or released extracellularly [16] as a response to a multitude of stressors. The metabolites can be analysed by the Liquid Chromatography-Mass Spectrometry-Electrospray Ionization (LC-MS-ESI) which is the common separation technique for the MS-based metabolomics to identify a large portion of the metabolites [17].

Microalgae are versatile as the source of lipid for biofuel, and value-added bioactive compounds, and are easy to grow in short cultivation time. Marine microalgal species such as *Nannochloropsis oculata*, is rich in polyunsaturated fatty acids (PUFA) (especially omega-3), proteins, and pigments including violaxanthin. *N. oculata* has been utilized as a feed in aquaculture, with big potential for biofuel production, environmental remediation and high-value biochemicals [18, 19, 20, 21]. Marine *Tetraselmis suecica* is rich in carotenoids, chlorophyll, α-Tocopherol, and other vitamins, and has been mostly used as a portion of live food for shrimp larvae, bivalves, artemia, and rotifers [22]. Fresh water *Chlorella vulgaris* is used as food additive and in pharmaceutical applications, and is rich in nucleic acid, protein, chlorophylls, carotenoids, minerals, vitamins (B12), and carbohydrate content [23]. The high cytotoxicity of the AgNPs on the Vero, MCF-7, and 4T1 cells has been reported. However, the AgNPs, in co-application with the *T. suecica*-CHL at the 2:1 ratio, have exhibited no toxicity on the Vero cells, though the cytotoxicity on the MCF-7 and 4T1 cells are retained [7]. The effects of elevated levels of AgNPs with the MCEs from W and ETH extracts (AgNPs-MCEs-W and ETH) at the 3:1, 4:1 and 5:1 ratios, on the non-cancerous and cancerous cells, have not been reported before. This study was based on the hypothesis that the elevated level of the AgNPs should be more cytotoxic to both the cancerous and non-cancerous cells. The presence of microalgal natural compounds from the green solvent extracts; or the MCEs rich in antioxidant activities, could reduce the toxicity of the elevated AgNPs level on the non-cancerous cells, whilst retaining the cytotoxicity on the cancerous cells.

The objectives of this study were to determine the cytotoxicity of the elevated AgNPs as the model heavy metal contaminants, in the presence of *N. oculata*, *T. suecica* and *Chlorella* sp.-W, ETH and CHL, at the 3:1, 4:1 and 5:1 ratios (AgNPs:MCEs, v/v), against the non-cancerous Vero cells, and the cancerous MCF-7 and 4T1 cells. The cytotoxic activities were confirmed with the flow cytometric and apoptotic biomarker analyses. The bioactive compounds of the MCEs-W and ETH were analysed by the LC-MS-ESI technique, and compared with the different solvent extracts from CHL, HEX, and MET.

2. Materials and methods

2.1. Cultivation and extraction of microalgae

The cultivation and extraction of microalgae have been described before [7]. The *N. oculata, T. suecica* and *Chlorella* sp., used in the present study, were morphologically characterized, and taxonomically identified by the Fisheries Research Institute of Malaysia, Kuala Muda, Kedah, Malaysia, under the guidance of Dr. Mohd Fariduddin Othman. The *N. oculata* species was further molecularly identified by using the 18S rRNA, rbcL gene, and the internal transcribed spacer (ITS) region of the ribosomal RNA transcription units. The partial 18S rRNA sequence, partial rbcl gene, and ITS region were determined, showing 97–99% similarity to *Nannochloropsis oculata*, as confirmed by the sequence alignment and phylogenetic tree analysis, and deposited into the GenBank with accession numbers HQ201714, HQ201713, and HQ201712, respectively [24]. The extraction of microalgae was as being reported before [7].

2.2. Preparation of AgNPs-MCEs ratio

The detail of the biosynthesis and characterization of AgNPs, and the isolation, identification and culture of *Lactobacillus plantarum* for AgNPs biosynthesis have been described elsewhere [8].

For the preparation of the AgNPs:MCEs ratio, 10 mg of AgNPs were dissolved in 1 ml of dimethylsulfoxide (DMSO) (10 mg/ml stock), and 10 mg of MCEs-CHL, ETH and W were dissolved in 1 ml DMSO (10 mg/ml stock). Various concentrations of AgNPs and MCEs were prepared (3.125–100 μg/ml) for single applications. For co-applications, each stock solution of AgNPs and MCEs was mixed to give the final total concentration of 10 mg/ml at 3:1, 4:1 and 5:1 ratios (AgNPs:MCEs (w/w)) (Table 1). The Eco-AlgaeAgNano™-W and ETH were compared with the AgNPs-MCEs-CHL. Preliminary studies on the MCEs-MET and HEX (data not shown) showed no significant cytotoxicity on the MCF-7 and 4T1 cells, while the MCEs-CHL showed moderate cytotoxicity. So, subsequent studies were based on the comparison between the MCEs-CHL and MCEs-W and ETH. The ratios of 3:1, 4:1 and 5:1 were selected based on the preliminary studies carried out with the 1:1, 1.5:1, 2:1, 1.5:3 ratios (data not shown). The highest ratio at 2:1 was cytotoxic against the MCF-7 cells, but exhibited very low or no cytotoxicity against the 4T1 cells.

2.3. In vitro cytotoxicity assay

2.3.1. Cell lines

The MCE-7 (ATCC® HTB-22T^{M}) and Vero cells (ATCC® CCL-81™) were obtained from the Institute of Marine Biotechnology, Universiti Malaysia Terengganu, Terengganu, Malaysia, while the 4T1 cells were from ATCC (ATCC® CRL-2539™). The Vero cells are the most common mammalian continuous cell line used in research and suitable for the screening assays of natural products, *in vitro* studies [25, 26, 27, 28, 29, 30], and are usually used in cancer studies as normal cell lines [27]. Vero cells have been tested extensively in the production of the vaccine and found to be free from the symptomatic agents which could have reduced the sensitivity of the tests. The cell-line does not produce tumors at the passage level used to form the vaccine but could have had the possibility of spreading tumor at much higher passage level [31, 32]. The progeny of Vero cells is aneuploid and continuous, which contains an abnormal number of chromosomes. A persistent cell lineage can be replicated through numerous cycles of mitosis and does not become aging [33]. Vero cells are interferon-deficient, and unlike the normal mammalian cells, they do not secrete α- or β-interferon (IFN) when infected with

Table 1. Preparation of AgNPs-MCEs co-application ratio.

Ratio	AgNPs (Stock 10 mg mL^{-1})	MCE (Stock 10 mg mL^{-1})	Total volume	Volume per well	Concentration
3:1	45 μL	15 μL	5,940 μL	6 mL	100 μg/mL, serial dilution to 50, 25, 12.5, 6.25, 3.125, 0 μg/mL
4:1	48 μL	12 μL	5,940 μL	6 mL	
5:1	50 μL	10 μL	5,940 μL	6 mL	

viruses. However, they still have an α/β IFN receptor, and exhibit responses when the recombinant IFN is added to the culture media [34]. The Vero cells are therefore used in this study as the normal cell line control due to this susceptibility to different types of chemical compounds, microbes, and toxins.

2.3.2. Cell culture

The Minimum Essential Medium (MEM) supplemented with 10% Fetal Bovine Serum (FBS), 1% sodium pyruvate, 1% penicillin streptomycin and 1% Non-essential amino acid was used for the culture of MCF-7 and Vero cells. The Roswell Park Memorial Institute (RPMI)-1640 medium supplemented with 10% FBS 100 unit/ml penicillin and 100 mg/ml streptomycin without phenol red, and 2 mM L-glutamine was used to culture 4T1 cells. The cells were maintained in a humidified atmosphere, containing 5% CO_2 and at 37 °C. The media was changed every 2–3 days, by replacing the old media with the fresh one. Trypsin-EDTA was used to trypsinize the cells for cell counting to assess the viability, proliferation, and confluency.

2.3.3. MTT assay

The MTT (3-(4,5-dimethylthiazol-2-yl)-2,5-diphenyltetrazolium bromide) assay is based on the ability of a mitochondrial dehydrogenase enzyme in the viable cells to cleave the tetrazolium rings of the pale yellow MTT and form formazan crystals in purple color [35]. The number of surviving cells therefore is directly proportional to the level of the formed formazan [36]. The cytotoxicity of the AgNPs and MCEs single and co-application on the MCF-7 (5×10^4) and 4T1 (2×10^4) and Vero (4×10^4) cells were assayed after 24, 48 and 72 h. One hundred μL of the cell suspension were pipetted into each of the 96-well plate, to allow cell attachment and proliferation. After overnight incubation, the cells were treated with various concentrations (3.125–100 μg/ml) of MCEs and AgNPs for single and co-applications. Each well was subjected to an MTT assay following the previously reported methods [7, 37].

2.3.4. Morphological characterization

The MCF-7, 4T1 and Vero cells were seeded for 24 h and the media was later changed with the fresh media containing AgNPs and MCEs at the IC_{50} levels established for 72 h treatment. The negative Control was without treatment. The cell morphology was observed under inverted microscope.

2.4. Flow cytometric analyses

2.4.1. Determination of apoptosis

Flowcytometric analyses were carried out to determine whether the cell death in breast cancer and Vero cells was due to apoptosis or necrosis. The MCF-7, 4T1 and Vero cell were cultured in 75 cm^3 flasks for 24 h, and then treated with the AgNPs-MCEs single and co-application. After 24 h, the cells were harvested by trypsinization and then resuspended in 1 ml Binding buffer and centrifuged at 300×*g* for 10 min. The cell pellet was re-suspended in 100 μL of 1× Binding Buffer (per 10^6 cells). Ten μL of fluorescence labeled Annexin V-FITC was loaded per 10^6 cells, mixed well and incubated for 15 min in the dark at room temperature. The cells were washed by adding 1 ml of 1× Binding Buffer per 10^6 cells and centrifuged at 300×*g* for 10 min. The cell pellet was re-suspended in 500 μL of 1× Binding Buffer per 10^6 cells. Finally, 5 μL of Propidium iodide (PI) solution was added immediately prior to flow cytometric analysis (Beckman Coulter CytoFLEX, USA). The negative Controls were the untreated cells [7]. The Phosphatidylserine (PS) levels, expressed in Relative Fluorescence Unit (RFU) in the cells from the untreated Controls, served as a baseline indicator for normal PS levels [38].

2.4.2. Cell-cycle analysis

The method used was as described before [7]. The breast cancer and Vero cells were cultured in 75 cm^3 flasks and incubated for 24 h. After incubation, the cells were harvested by trypsinization and then resuspended with 1 ml of PBS addition and centrifugation at 1200 rpm and 4 °C. The pelleted cells were re-suspended in 0.3 ml of PBS buffer. The cells (1×10^6) were fixed by gently adding 700 μL of cold ethanol (70%) drop wise to the tube containing 300 μL of cell suspension in PBS, and vortexed gently. The fixed cells in the tube were left on ice for 1 h (or a few days at 4 °C), centrifuged, washed 1 time with cold PBS, re-centrifuged, and the cell pellet re-suspended in 250 μL of PBS. Five μL of 10 mg/ml RNAse A was added (the final concentration being 0.2–0.5 mg/ml). After incubation at 37 °C for 30 min, ten μL of 1 mg/ml PI solution was added (the final concentration being 10 μg/ml). Finally, the sample was kept in the dark at 4 °C until analysis by flow cytometry.

2.5. Apoptotic biomarkers

2.5.1. ADP/ATP ratio

The procedure was carried out as previously described [7]. The breast cancer and Vero cells were cultured on white 96-well plates at 10^4 cells/well for 24 h and then treated with desired apoptosis inducer (including the untreated cells). After 24 and 48 h, the culture medium was removed from the plate, 50 μL of Nucleotide Releasing Buffer (10^3–10^4 cells) was added to help gently loosen the membrane, so that the ATP will leak out of the cell without complete cell lysis, and incubated for 5 min at room temperature with gentle shaking. One hundred μL of ATP Monitoring Enzyme was added to the Control and the sample in the white 96-well plate. and the background luminescence (Data A) was read. Fifty μL of cells were transferred into the luminometer plate and treated with the Nucleotide Releasing Buffer. After 5 min, the sample in the luminometer or luminescence capable plate reader (Data B) was read, and then the sample was read after 10 min incubation at room temperature (Data C). Later, the 10X ADP-Converting enzyme was diluted 10-fold with the Nucleotide Releasing Buffer, and 10 μL of 1X ADP Converting Enzyme was added. The samples were again read after 5 min (Data D). The data was analysed as follows:

$$\text{ADP / ATP ratio} = [\text{Data D} - \text{Data C}] / [\text{Data B} - \text{Data A}] \quad (1)$$

Data D = Sample signal 5 min after the addition of 10 μL 1X ADP Converting Enzyme to the cells.
Data C = Sample signal prior to the addition of 1X ADP Converting Enzyme to the cells.
Data B = Sample signal 5 min after the addition of cells to the reaction mix
Data A = Background signal of the reaction mix.

2.5.2. Caspase 3/7

Caspase 3/7 (effector caspases) is related to the onset of the "death cascade" and are responsible for initiating the degradation stage of apoptosis such as DNA fragmentation, cell contraction and membrane blebbing [39]. It thus signifies the important cell entry point into the

apoptotic signaling pathway [40]. The breast cancer and Vero cells were cultured on the white 96-well plate for 24 h. Then, the cells (2×10^4) were treated with the MCEs-AgNPs at the IC_{50} values, and incubated for 24 and 48 h. In a 96 well plate, 100 μL of Caspase-Glo® 3/7 reagent was added to each well of the white 96-well plate containing 100 μL of the blank, negative Control cells or treated cells in the culture medium, and the plate was agitated for 30 s. The plate was then incubated for 30 min to 3 h at room temperature in the dark, and the luminescence of each sample was measured in a plate-reading luminometer (GloMax® System, Promega, USA) according to the manufacturer's protocol, as described before [7].

2.6. Identification of compounds by Liquid Chromatography–Mass Spectrometry-Electrospray Ionization (LC-MS-ESI)

The MCEs were analyzed using a LC-MS (LCMS-IT-TOF, SHIMADZU, Japan), equipped with an electrospray ionization interface in the positive and negative mode. The separation was performed in a SunFire C18 column (150 mm × 2.2 mm × 3.5 μm, Waters, Milford, MA) using the gradient solvent system (Table 2) as follows: - Solvent A (acetonitrile, 0.1% formic acid) and Solvent B (water, 0.1% formic acid). The flow rate was set at 0.2 ml/min, and the injection volume was 20 μL, 13 L/min dry gas flow (N_2), 30 psi nebulizer pressure, 350 °C drying gas temperature, and 4500 V capillary voltage. The full-scan MS was recorded for 400–700 *m/z*. The raw data was first transferred into centroid mode data of mzXML format using MSConvert tool from Proteowizard software (http://proteowizard.sourceforge.net/). The metabolites were identified and further confirmed by comparing the retention time and the MS spectra with the commercially available standard or matching the accurate mass information with the online Metabolomics Workbench database (www.metabolomicsworkbench.org), METLIN (metlin.scripps.edu) and HMDB (www.hmdb.ca).

2.7. Statistical analysis

All experiments were carried out in triplicate and the results were expressed as the means ± standard deviation (SD). Two-way ANOVA model was used for the analysis of statistical significance by using GraphPad Prism software (version 6, CA, USA), and a $p < 0.05$ threshold was considered to indicate the significant differences (Tukey's test).

3. Results

3.1. Cytotoxicity of AgNPs-MCEs

Table 3, and Figures 1 and 2 show the cytotoxic effects of AgNPs-MCEs–W, ETH and AgNPs-MCEs-CHL on Vero, MCF-7 and 4T1 cell-lines, at the 3:1, 4:1, and 5:1 ratios (AgNPs:MCEs), after 24, 48 and 72 h treatments. For the AgNPs-MCEs-W, the IC_{50} values were 83.17–95.49 and 70.79–91.20 μg/mL on Vero cells; 13.18–28.18 and 12.58–25.7 μg/ml on MCF-7; and 16.21–33.88 and 14.79–26.91 μg/ml on 4T1 cells, after 48 and 72 h treatment, respectively. For ETH at the 4:1 and 5:1 ratios, the IC_{50} values after 48 and 72 h treatment were 63.09–91.2 and 56.23–89.12 μg/ml on Vero cells; 13.48–26.61 and 10.47–19.95 μg/ml on MCF-7; and 15.13–58.88 and 14.12–50.11 μg/ml on 4T1 cells, respectively. Based on this, the AgNPs-MCEs-W exhibited better performance than the AgNPs-MCEs-ETH. For 24 h treatment, the AgNPs-*Chlorella* sp.-W and ETH formulation at the 4:1 and 5:1 ratios showed reduced cytotoxicity at the IC_{50} of 89.12–95.49 μg/ml on Vero cells, as compared to 18.62–22.38 μg/ml on MCF-7 cells, and 21.37–25.70 μg/ml on 4T1 cells (Table 3). For comparison, after 24, 48 and 72 h treatment, the AgNP single application exhibited the IC_{50} of 35.48, 30.19 and 25.11 μg/ml on Vero cells; 23.98, 7.36 and 5.31 μg/ml on MCF-7 cells; and 19.95, 19.05 and 17.78 μg/ml on 4T1 cells, respectively [8]. The *Chlorella*-CHL was non-cytotoxic on the Vero cells and showed moderate to low cytotoxicity with the IC_{50} of 52.48 and 39.81 μg/ml on MCF-7 cells after 48 and 72 h, respectively; and 83.17 μg/ml on 4T1 cells after 72 h [8].

The AgNPs-MCEs-CHL at the 4:1 and 5:1 ratio similarly exhibited low cytotoxicity after 48 and 72 h treatment at the IC_{50} of 51.28–75.85 and 48.97–69.18 μg/ml on Vero cells; but higher cytotoxicity against MCF-7 cells at IC_{50} of 10.47–16.98 and 6.19–14.45 μg/ml, and 15.84–31.62 and 12.58–24.54 μg/ml on 4T1 cells, respectively. After 24 h treatment, the AgNPs-MCEs-CHL at the 4:1 and 5:1 ratios showed low cytotoxicity at IC_{50} of 54.95–87.09 μg/ml on Vero cells, but high cytotoxicity with IC_{50} of 12.58–19.95 μg/ml on MCF-7 cells, and 22.38–37.15 μg/ml on 4T1 cells. After 24 and 48 h treatments, the AgNPs-MCEs-CHL exhibited higher cytotoxicity on MCF-7 and Vero cells, but at lower than or with comparable cytotoxicity on 4T1 cells especially to the AgNPs-MCEs-W. After 72 h, the AgNPs-*Chlorella* sp.-ETH showed comparable cytotoxicity to the AgNPs-*Chlorella* sp.-CHL ($p > 0.05$) on MCF-7 cells, while the AgNPs-MCEs-W and ETH showed more significant cytotoxicity than the AgNPs-MCEs-CHL on 4T1 cells ($p < 0.05$). The criteria of cytotoxicity for the crude extract and AgNPs against MCF-7, 4T1 and Vero during the preliminary assay, based on the IC_{50} values are as follows [41, 42]: $IC_{50} \leq$ 20 μg/mL = high cytotoxicity, IC_{50} 21–45 μg/ml = moderate cytotoxicity, IC_{50} 46–100 μg/ml = low cytotoxicity, and $IC_{50} > 100$ μg/ml or no IC_{50} estimated = non-cytotoxic (as shown in Table 3). All the co-application formulations had exhibited much lower or reduced cytotoxic effects on the Vero cells, as compared to the single AgNPs ($p <$ 0.05).

Table 2. The solvent for gradient system.

Time (min)	Solvent A (%)	Solvent B (%)
0–5	70	30
6–10	80	20
11–15	90	10
16–20	95	5
21–35	100	0

3.2. Apoptotic and cell-cycle analyses

The untreated (control) cells showed intact and regular shape. The cells appeared large, rounded, healthy looking and attached to each other, with no apoptotic bodies or necrotic cells (Figure 3). The AgNPs-MCEs–W and ETH treatments did not exhibit any significant changes in the morphology and survival of the non-cancerous Vero cell line (Figure 4). The AgNPs-MCEs treatment however had resulted in cell morphological changes in MCF-7 and 4T1 cells where the cells became rounded up, shrinking in size, and detached from the monolayer surface of the wells (as shown by the arrows) (Figures 5 and 6). The number of cells was also lower than the Control, with some cells showing membrane blebbing and the formation of apoptotic bodies observed as round or oval masses of cytoplasm, much smaller than the original cells. These are the initial characteristic features of apoptotic cell death.

To confirm the induction of apoptosis after 24 h treatment with the AgNPs-MCEs–W, ETH and AgNPs-MCEs-CHL, Annexin V analysis was carried out to determine the viable, early apoptotic, late apoptotic, and necrotic cells [27, 35]. The AgNPs-*N. oculata*-CHL (5:1) (42.26%) exhibited the highest late apoptosis in MCF-7 cells, followed by AgNPs-*T. suecica*-W (5:1) (35.02%), and AgNPs-*Chlorella* sp.-CHL and W (33.52%) (5:1). The early apoptosis was significantly increased with the AgNPs-*T. suecica*-CHL (36.73%), AgNPs-*Chlorella* sp.-CHL (25.82%), and AgNPs--*Chlorella* sp.-ETH (22.18%) at the 5:1 ratio (Figure 7a). The highest cytotoxic activity of the AgNPs-*T. suecica*-CHL and AgNPs-*N. oculata*-CHL (5:1) co-application on MCF-7 cells may be due to enhanced apoptotic induction, as compared to the Control, other formulation and single applications. For 4T1 cells (Figure 7b), the highest late apoptosis was achieved with AgNPs-*Chlorella* sp.-ETH (39.26%), AgNPs-*Chlorella* sp.-CHL (36.32%), AgNPs-*T. suecica*-W (33.49%), and AgNPs-*T.*

Table 3. IC_{50} values of AgNPs-MCEs–W, ETH formulation, in comparison to AgNPs-MCEs-CHL, on Vero, MCF-7 and 4T1 cell-lines (Tamoxifen is the positive control [83]; The untreated cells are the negative control).

Cell-lines/Co-application ratio (w/w)	24 h			48 h			72 h		
	3:1	4:1	5:1	3:1	4:1	5:1	3:1	4:1	5:1
Vero									
Tamoxifen	11.22 ± 0.01								
Negative control	>100	>100	>100	>100	>100	>100	>100	>100	>100
AgNPs-*N. oculata*-ETH	>100	>100	95.49 ± 0.04	>100	>100	91.20 ± 0.05	>100	>100	89.12 ± 0.03
AgNPs-*N. oculata*-W	>100	100 ± 0.05	97.7 ± 0.04	>100	95.49 ± 0.03	95.49 ± 0.06	100 ± 0.03	91.20 ± 0.02	89.12 ± 0.07
AgNPs-*N. oculata*-CHL	100 ± 0.02	85.11 ± 0.02	79.43 ± 0.02	77.62 ± 0.03	75.85 ± 0.03	69.18 ± 0.02	75.85 ± 0.04	69.18* ± 0.02	67.60* ± 0.03
AgNPs-*T. suecica*-ETH	100 ± 0.04	91.20 ± 0.02	74.13 ± 0.02	87.09 ± 0.03	66.06* ± 0.01	63.09* ± 0.04	81.2 ± 0.06	64.56** ± 0.03	56.23*** ± 0.03
AgNPs-*T. suecica*-W	100 ± 0.01	95.49 ± 0.02	87.09 ± 0.01	91.20 ± 0.02	87.09 ± 0.01	83.17 ± 0.04	79.43 ± 0.03	75.85 ± 0.03	70.79 ± 0.03
AgNPs-*T. suecica*-CHL	89.12 ± 0.01	87.09 ± 0.21	70.79 ± 0.01	70.79 ± 0.02	66.06* ± 0.02	53.70* ± 0.02	69.18* ± 0.03	61.65** ± 0.03	50.11*** ± 0.02
AgNPs-*Chlorella* sp.-ETH	>100	95.49 ± 0.02	93.32 ± 0.05	>100	91.20 ± 0.04	85.11 ± 0.04	>100	81.28 ± 0.02	72.44 ± 0.02
AgNPs-*Chlorella* sp.-W	100 ± 0.02	95.49 ± 0.02	91.20 ± 0.06	100 ± 0.05	89.12 ± 0.03	85.11 ± 0.04	95.49 ± 0.06	83.17 ± 0.07	74.13 ± 0.02
AgNPs-*Chlorella* sp.-CHL	67.6* ± 0.04	61.65* ± 0.02	54.95* ± 0.01	53.70* ± 0.02	52.48** ± 0.03	51.28** ± 0.02	52.48*** ± 0.04	50.11*** ± 0.01	48.97*** ± 0.20
MCF-7									
Tamoxifen	12.2 ± 0.02								
Negative control	>100	>100	>100	>100	>100	>100	>100	>100	>100
AgNPs-*N. oculata*-ETH	70.79 ± 0.02	38.01 ± 0.01	31.62 ± 0.01	54.95 ± 0.03	26.91* ± 0.03	21.37* ± 0.03	28.18*** ± 0.02	19.95** ± 0.02	19.05** ± 0.01
AgNPs-*N. oculata*-W	35.48 ± 0.03	33.11 ± 0.02	27.54* ± 0.02	31.62 ± 0.02	28.18 ± 0.01	23.98* ± 0.02	28.84*** ± 0.03	25.70** ± 0.02	19.95** ± 0.02
AgNPs-*N. oculata*-CHL	19.05** ± 0.02	19.05** ± 0.01	18.62** ± 0.02	16.21* ± 0.02	15.13** ± 0.01	13.48** ± 0.02	11.22*** ± 0.02	10.00*** ± 0.04	9.81*** ± 0.02
AgNPs-*T. suecica*-ETH	35.48 ± 0.01	34.67 ± 0.01	33.88 ± 0.01	20.89* ± 0.06	19.49* ± 0.05	13.48** ± 0.02	17.37* ± 0.01	15.13** ± 0.01	12.58*** ± 0.06
AgNPs-*T. suecica*-W	25.11* ± 0.03	19.95** ± 0.03	15.84** ± 0.01	19.95* ± 0.04	16.59* ± 0.01	13.18** ± 0.04	19.05** ± 0.02	13.48** ± 0.01	12.58*** ± 0.01
AgNPs-*T. suecica*-CHL	15.13** ± 0.03	12.88** ± 0.02	12.58** ± 0.02	13.48** ± 0.02	11.74** ± 0.01	10.47** ± 0.02	11.22*** ± 0.03	6.56**** ± 0.02	6.19**** ± 0.02
AgNPs-*Chlorella* sp.-ETH	25.11* ± 0.01	20.41** ± 0.03	19.05** ± 0.01	21.37* ± 0.03	16.59* ± 0.01	16.59* ± 0.04	16.98* ± 0.02	15.84** ± 0.01	10.47*** ± 0.02
AgNPs-*Chlorella* sp.-W	24.54* ± 0.01	22.38** ± 0.03	18.62** ± 0.01	22.90 ± 0.03	19.49* ± 0.01	17.37* ± 0.04	20.41* ± 0.02	18.62 ± 0.01	15.13** ± 0.02
AgNPs-*Chlorella* sp.-CHL	23.44* ± 0.03	19.95** ± 0.02	18.62** ± 0.02	21.87** ± 0.01	16.98** ± 0.03	15.84** ± 0.02	16.98* ± 0.04	14.45** ± 0.04	9.44**** ± 0.02
4T1									
Tamoxifen	5.05 ± 0.01								

(*continued on next page*)

Table 3 (*continued*)

Cell-lines/Co-application ratio (w/w)	24 h			48 h			72 h		
	3:1	4:1	5:1	3:1	4:1	5:1	3:1	4:1	5:1
Negative control	>100	>100	>100	>100	>100	>100	>100	>100	>100
AgNPs-*N. oculata*-ETH	74.13 ± 0.04	67.6 ± 0.06	51.28 ± 0.01	63.09 ± 0.01	58.88 ± 0.02	47.86 ± 0.05	56.23*** ± 0.02	50.11 ± 0.06	43.65 ± 0.02
AgNPs-*N. oculata*-W	43.65 ± 0.01	38.01 ± 0.02	31.62 ± 0.01	39.81* ± 0.02	26.30* ± 0.02	22.90** ± 0.02	36.30 ± 0.03	19.95*** ± 0.06	18.19**** ± 0.05
AgNPs-*N. oculata*-CHL	41.68 ± 0.02	37.15 ± 0.02	32.35 ± 0.03	36.30** ± 0.03	31.62** ± 0.03	26.91*** ± 0.03	31.62** ± 0.03	24.54*** ± 0.03	19.05**** ± 0.03
AgNPs-*T. suecica*-ETH	50.11 ± 0.02	44.66 ± 0.02	30.19 ± 0.01	41.68 ± 0.02	25.11*** ± 0.02	22.38**** ± 0.02	30.19** ± 0.04	18.62**** ± 0.04	16.98**** ± 0.02
AgNPs-*T. suecica*-W	41.68 ± 0.02	38.01 ± 0.02	35.48 ± 0.01	37.15* ± 0.02	33.88* ± 0.02	27.54*** ± 0.02	30.19** ± 0.04	26.91** ± 0.04	23.98*** ± 0.02
AgNPs-*T. suecica*-CHL	38.90 ± 0.02	33.88 ± 0.02	26.91* ± 0.01	28.18* ± 0.03	26.91** ± 0.01	23.98*** ± 0.03	21.87*** ± 0.06	22.38*** ± 0.06	19.95*** ± 0.02
AgNPs-*Chlorella* sp.-ETH	26.91* ± 0.02	21.37* ± 0.01	21.37* ± 0.01	21.37** ± 0.07	16.59*** ± 0.03	15.13**** ± 0.01	20.89*** ± 0.04	15.84**** ± 0.04	14.12**** ± 0.03
AgNPs-*Chlorella* sp.-W	27.54* ± 0.02	25.70* ± 0.02	22.38** ± 0.01	20.89**** ± 0.02	18.62**** ± 0.02	16.21**** ± 0.02	18.19**** ± 0.04	15.84**** ± 0.04	14.79**** ± 0.02
AgNPs-*Chlorella* sp.-CHL	39.81 ± 0.02	35.48 ± 0.02	22.38** ± 0.01	30.19*** ± 0.02	25.11*** ± 0.03	15.84**** ± 0.02	19.95*** ± 0.02	19.49**** ± 0.02	12.58**** ± 0.02

NB: Data expressed as mean ± standard deviation ($n = 3$) for statistically significant difference between microalgae extracts, ratio and time exposure. Significant level: $0.010 < p \leq 0.05$, significant *; $0.001 < p \leq 0.010$, very significant**; and $p \leq 0.001$, highly significant ***.

suecica-CHL (32.5%) at the 5:1 ratio. The early apoptosis was the highest with AgNPs-*Chlorella* sp.-W (21.55%), AgNPs-*T. suecica*-ETH (20.54%), AgNPs-*N. oculata*-W (19.04%), and AgNPs-*Chlorella* sp.-CHL (18.3%) (5:1). The AgNPs-*Chlorella* sp.-ETH and AgNPs-*Chlorella* sp.-CHL achieved the highest cytotoxicity against 4T1 cells. The early and late apoptosis events were increased with higher ratio of AgNPs in co-application, as compared to the single application of the AgNPs (16.33, 25.59%, respectively) and the MCEs (0.95–1.1, 2.7–6.3%, respectively) [8]. For Vero cells (Figure 7c), the highest early apoptosis was achieved with AgNPs-*Chlorella* sp.-CHL (7.43%), AgNPs-*N. oculata*-CHL (6.73%), AgNPs-*T. suecica*-ETH (6.61%) and AgNPs-*T. suecica*-CHL (5.27%), while the late apoptosis was higher with AgNPs-*T. suecica*-CHL (3.11%), and AgNPs-*Chlorella* sp.-CHL (2.71%) at 5:1 ratio. All the other treatments showed early and late apoptosis events similar to Control. This significant reduction in early and late apoptosis after the AgNPs-MCEs co-application treatment confirmed the lower cytotoxicity exhibited on the Vero cells (Figures 8 and 9), as compared to the single application of AgNPs.

Figure 10a shows significant increase in the sub-G1 phase (the apoptotic events) of MCF-7 cells after 24 h treatment, which was the highest with the AgNPs-*T. suecica*-CHL (5:1) (40.17%), followed by AgNPs-*Chlorella* sp.-CHL (5:1) (34.72%), AgNPs-*N. oculata*-CHL (5:1) (33.84%) and AgNPs-*Chlorella* sp.-ETH (5:1) (32.28%). Compared to 48% in Control, a significant drop to about 29–41% in all the AgNPs-MCEs co-application was observed for G1 phase, except with the AgNPs-*N. oculata*-ETH (64.57%). The event distribution in the S phase was decreased from 26% (Control) to 6.6–13.46% in all the treated cells, lower than the MCEs single application [8]. The G2/M phase showed significant drop in all the treated cells with co-application, as compared to the control, suggesting the cell cycle arrest through the reduction of the DNA synthesis or halting the mitosis. For 4T1 cell-lines (Figure 10b), the G1 phase was slightly decreased from 55% to 43–53%, the S phase also slightly decreased from 20% to 10–20%, and the G2/M phase decreased from 11% to 2–7% in all cells treated with AgNPs-MCEs co-application. However, the sub-G1 phase was highly increased with the AgNPs-*Chlorella* sp.-CHL (5:1) (36.54%), AgNPs-*Chlorella* sp.-ETH (5:1) (36.03%), AgNPs-*T. suecica*-ETH (5:1) (32.78%), AgNPs-*N. oculata*-W (5:1) (29.49%), and AgNPs-*N. oculata*-CHL (5:1) (28.9%), as compared to the Control (4%), MCEs (6–8%) and AgNPs (20.93%) single application [8]. The co-application also inhibited the cellular proliferation of 4T1 cells *via* the cell cycle arrest. For Vero cells (Figure 10c), the AgNPs-MCEs showed increased sub-G1 phase (8.99–11.51%) as compared to the Control (8.99%). These indications of apoptotic events were also lower than the AgNPs single application (15.11%) [8]. In comparison to the Control (70.4%), there was a decrease in the G0/G1 phase, especially with the AgNPs-*T. suecica*-CHL (5:1) (49.96%), AgNPs-*N. oculata*-ETH (5:1) (49.43%) and AgNPs-*Chlorella* sp.-CHL (5:1) (48.65%), attributable to the preparation for mitosis. As shown in Figures 11 and 12 for Vero cells, there was also a slight increase in S and G2/M phase (13.97–20.63% and 15.12–16.69%, respectively) than the Control (13.85), but still higher than the AgNPs (16.69%), indicating the continuous DNA synthesis. The co-application therefore exhibited the ability to reduce the toxicity of the AgNPs against Vero cell with reduced apoptosis, and increased DNA synthesis and mitosis.

3.3. Apoptotic biomarkers

Significant increase in ADP/ATP ratio in the MCF-7 cells was observed after treatment with AgNPs-MCEs-CHL, ETH, and W for 24 and 48 h (Figure 13a). The highest ratio was achieved, respectively, with the AgNPs-*T. suecica*-CHL (5:1) (3.5, 6.9), AgNPs-*Chlorella* sp.-CHL (5:1) (2.9, 5.8), AgNPs-*N. oculata*-CHL (5:1) (2.8, 5.5), and AgNPs-*Chlorella* sp.-ETH (5:1) (2.6, 5.3). The ADP/ATP ratios for other co-applications were between 1.9-2.4 and 5.05–4.04, respectively, and these were significantly ($p < 0.05$) higher than the Control (1, 1.8), AgNPs (1.9, 2.8) and MCEs (1.3–2.4, 3.2–4.8) single application after 24 and 48 h, respectively [8].

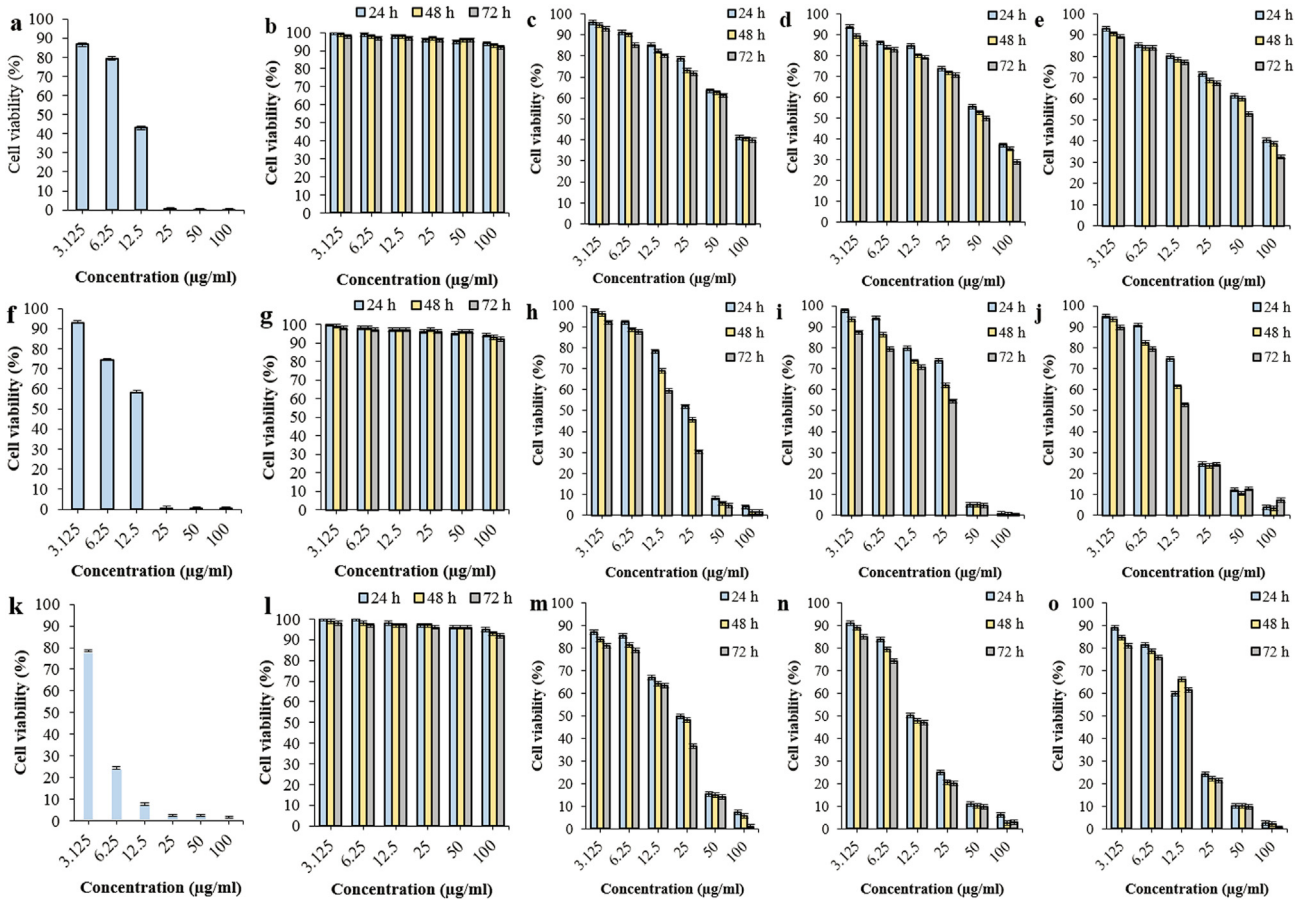

Figure 1. Cytotoxic effects after 24, 48 and 72 h treatment on i- Vero cells from (a) Positive control; (b) Negative control; (c) AgNPs-*N. oculata*-W; (d) AgNPs-*T. suecica*-W; (e) AgNPs-*Chlorella* sp.-W; ii- MCF-7 cells from (f) Positive control; (g) Negative control; (h) AgNPs-*N. oculata*-W; (i) AgNPs-*T. suecica*-W; (j) AgNPs-*Chlorella* sp.-W; iii- 4T1 cells from (k) Positive control; (l) Negative control; (m) AgNPs-*N. oculata*-W; (n) AgNPs-*T. suecica*-W; (o) AgNPs-*Chlorella* sp.-W at the 5:1 ratios (Positive control: Tamoxifen treatment; Negative control: Untreated cells).

However, the ADP/ATP ratio can be used as a complementary method and as an indicator of apoptosis, but not to give the actual level of induction. The higher ratio in the MCEs than the AgNPs after 48 h may suggest that it gives better indication of the late apoptosis. For 4T1 cells (Figure 13b), the AgNPs-*Chlorella* sp.-CHL (5:1) exhibited the highest ADP/ATP ratio (3.8, 6.5) after 24 and 48 h treatments, followed by AgNPs-*Chlorella* sp.-ETH (5:1) (3.7, 5.9), AgNPs-*Chlorella* sp.-W (5:1) (3.5, 5.86), and AgNPs-*N. oculata*-CHL (5:1) (3, 5.84), as compared to the Control (1, 1.3), respectively. For Vero cells, the AgNPs-MCEs co-application showed the ADP/ATP ratio similar to the control, suggesting the lower apoptosis, as compared to the AgNPs alone. The mechanism involved in the enhanced ADP/ATP ratio of the MCEs with AgNPs may be attributed to the bonding reaction between the large surface area of the AgNPs and the active functional groups of the MCEs, such as hydroxyl and amino groups of the bioactive compounds in the microalgae.

The highest early apoptosis and apoptotic events in MCF-7 cells, as shown in Figures 7 and 10a, were confirmed by the highest Caspase activity (42×10^4, 67×10^4 RLU) of the AgNPs-*T. suecica*-CHL (5:1) treatment, followed by AgNPs-*Chlorella* sp.-CHL (5:1) (33×10^4, 48×10^4 RLU) and AgNPs-*N. oculata*-CHL (5:1) (31×10^4, 45×10^4 RLU), after 24 and 48 h treatments, respectively (Figure 14a). For 4T1 cells (Figure 14b), the highest Caspase activity was exhibited by the AgNPs-*Chlorella* sp.-CHL (5:1) (31×10^4, 37×10^4 RLU) (confirming the highest apoptotic events in sub G1 as shown in Figure 10b), AgNPs-*Chlorella* sp.-ETH (5:1) (29×10^4, 35×10^4 RLU), AgNPs-*Chlorella* sp.-W (5:1) (28×10^4, 34×10^4 RLU), AgNPs-*T. suecica*-ETH (5:1) (27×10^4, 32×10^4 RLU), AgNPs-*N. oculata*-W (5:1) (25×10^4, 30×10^4 RLU) and AgNPs-*N. oculata*-CHL (5:1) (24×10^4, 30×10^4 RLU), respectively. The Caspase activities were significantly enhanced after the co-application treatments as compared to the AgNPs and MCEs single application ($p < 0.05$). For Vero cells, all the cells treated with the AgNPs-MCEs–W, ETH showed caspase activities similar to the Control which reflected the reduced cytotoxic activities of the AgNPs-MCEs treatment ($p < 0.05$).

3.4. Metabolite profiling by LC-MS-ESI

Tables 4, 5, and 6 show the LC-ESI-MS analyses in negative and positive ionization mode of *N. oculata*, *T. suecica* and *Chlorella* sp.-CHL, HEX, MET, ETH and W extracts. Sixty-four metabolites in negative ions and 56 metabolites in positive ions belonging to the classes of fatty acids, sterol lipids, pigment, N-acyl- α amino acids and their derivatives, and benzonic acid esters were tentatively identified. In the absence of analytical standards, the compound identification and confirmation may depend on the chromatographic and spectral information like the spectra, retention time, the presence of fragment ion as reported in the previous studies, or available on-line databases such as Metabolomics Workbench (www.metabolomicsworkbench.org) or Metlin (metlin.scripps.edu). The microalgal metabolites identified and analysed in our study, including fatty acids, lipids, sterol, and natural pigments, are important as pharmaceutical agent and in nutrient-dense food industry [43].

3.4.1. Fatty acids

For negative ion mode, five metabolites were tentatively identified as fatty acids (Table 5) assigned as arachidoyl dodecanoate ($t_R = 29.29$) (m/z 479.48) and (+)-24-methyl-hexacosanoic acid ($t_R = 18.29$) (m/z

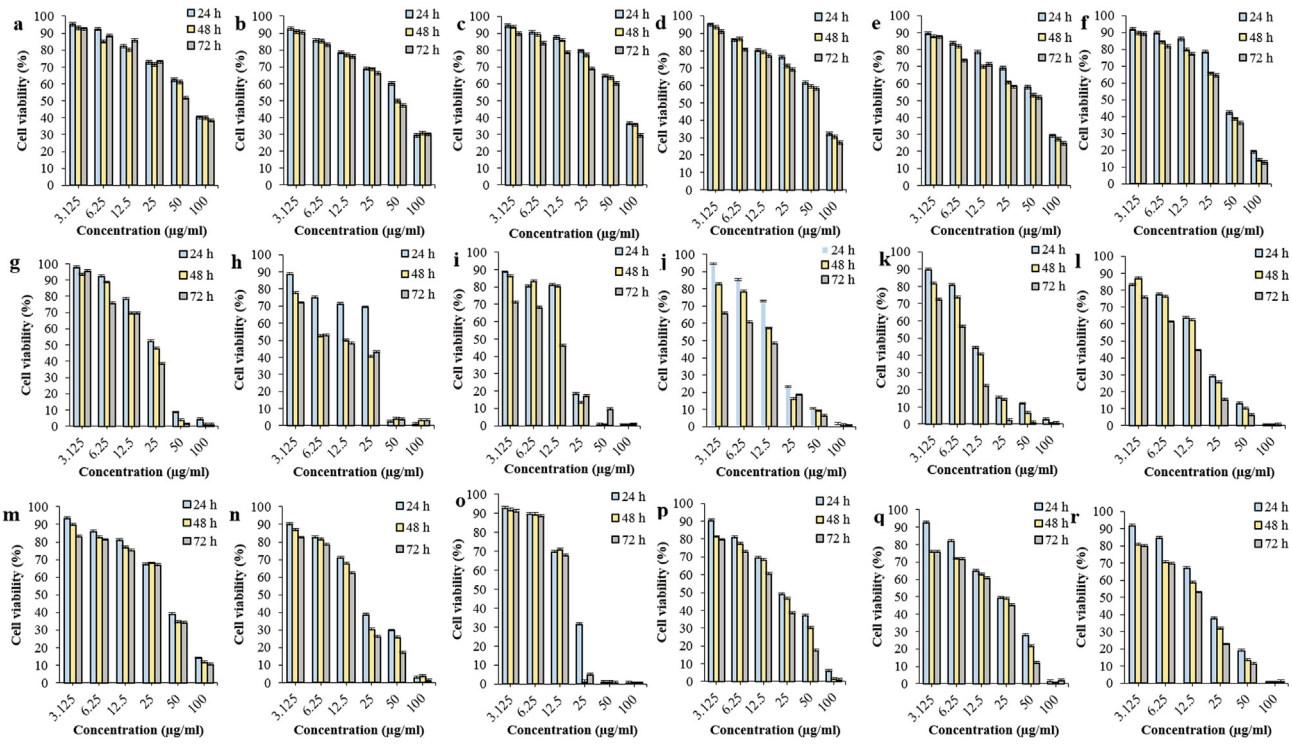

Figure 2. Cytotoxic effects at the 5:1 ratios of AgNPs-MCEs-ETH and AgNPs-MCEs-CHL after 24, 48 and 72 h treatment on i- Vero cells from (a) AgNPs-*N. oculata*-ETH; (b) AgNPs-*T. suecica*-ETH; (c) AgNPs-*Chlorella* sp.-ETH; (d) AgNPs-*N. oculata*-CHL; (e) AgNPs-*T. suecica*–CHL; (f) AgNPs-*Chlorella* sp.-CHL; ii- MCF-7 cells from (g) AgNPs-*N. oculata*-ETH; (h) AgNPs-*T. suecica*-ETH; (i) AgNPs-*Chlorella* sp.-ETH; (j) AgNPs-*N. oculata*-CHL; (k) AgNPs-*T. suecica*–CHL; (l) AgNPs-*Chlorella* sp.-CHL; iii- 4T1 cells from (m) AgNPs-*N. oculata*-ETH; (n) AgNPs-*T. suecica*-ETH; (o) AgNPs-*Chlorella* sp.-ETH; (p) AgNPs-*N. oculata*-CHL; (q) AgNPs-*T. suecica*–CHL; (r) AgNPs-*Chlorella* sp.-CHL.

410.40), detected in *N. oculata*-CHL, HEX, and *Chlorella* sp.-HEX. Table 4 shows that Stearidonoyl-CoA (t_R = 1.39) (*m/z* 544.94) was identified in MCEs-W, while Table 5 shows its presence in *T. suecica* and *Chlorella sp.*-MET, and *Chlorella* sp.-ETH. Stearoyl-CoA desaturase (SCD) which stimulates the de-saturation of D9-cis for a group of fatty acyl-CoA substrates, is the main and highly regulated enzyme required for the biosynthesis of mono-unsaturated fatty acids (MUFA) [44]. The metabolite octadecanoic acid trichloroethyl ester (t_R = 28.58) at *m/z* 414.18 was observed in MCEs-CHL and HEX but not detected in MCEs-MET, ETH and W, while octadecanoic acid trichloroethyl ester isomer (t_R = 32.08) was observed in MCEs-W and in all MCEs except *N. oculata*-CHL. For positive ion, three metabolites were identified as fatty acids (Table 6) – 22:6 Cholesteryl ester (t_R = 31.54) only in *N. oculata*-HEX; 22:6 Cholesteryl ester isomer (t_R = 32.83) at *m/z* 696.59 in MCEs-HEX, and *N. oculata*-CHL, ETH and *T. suecica*-MET, ETH and *Chlorella* sp.-MET; and 1-palmitoylglycerol 3-phosphate (t_R = 31.50) at *m/z* 411.25 in MCEs MET, ETH and *N. oculata* and *T. suecica*-CHL.

3.4.2. Sterol lipids, glycerolipids and triterpenoids

The negative ions mode identified 6 sterol lipids, 5 glycerol lipids, and 3 triterpenoids (Table 5). The steroid lipid 4 α hydroxymethyl-5 α -cholesta-8,24-dien-3β-ol (t_R = 26.75) at *m/z* 414.66 was found in MCEs-

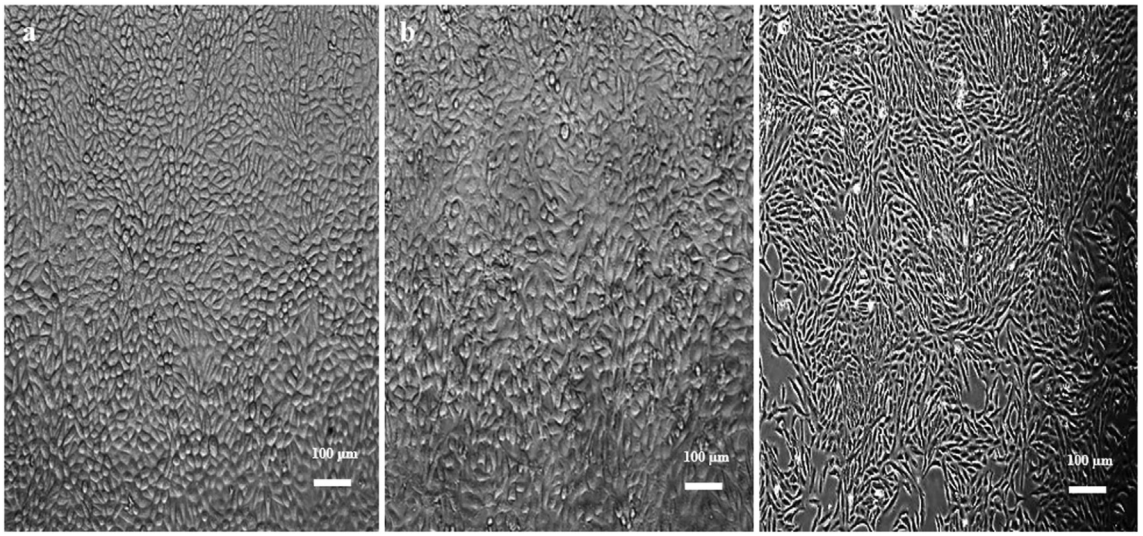

Figure 3. Morphological changes after 72 h of untreated (a) MCF-7; (b) 4T1; (c) Vero cells.

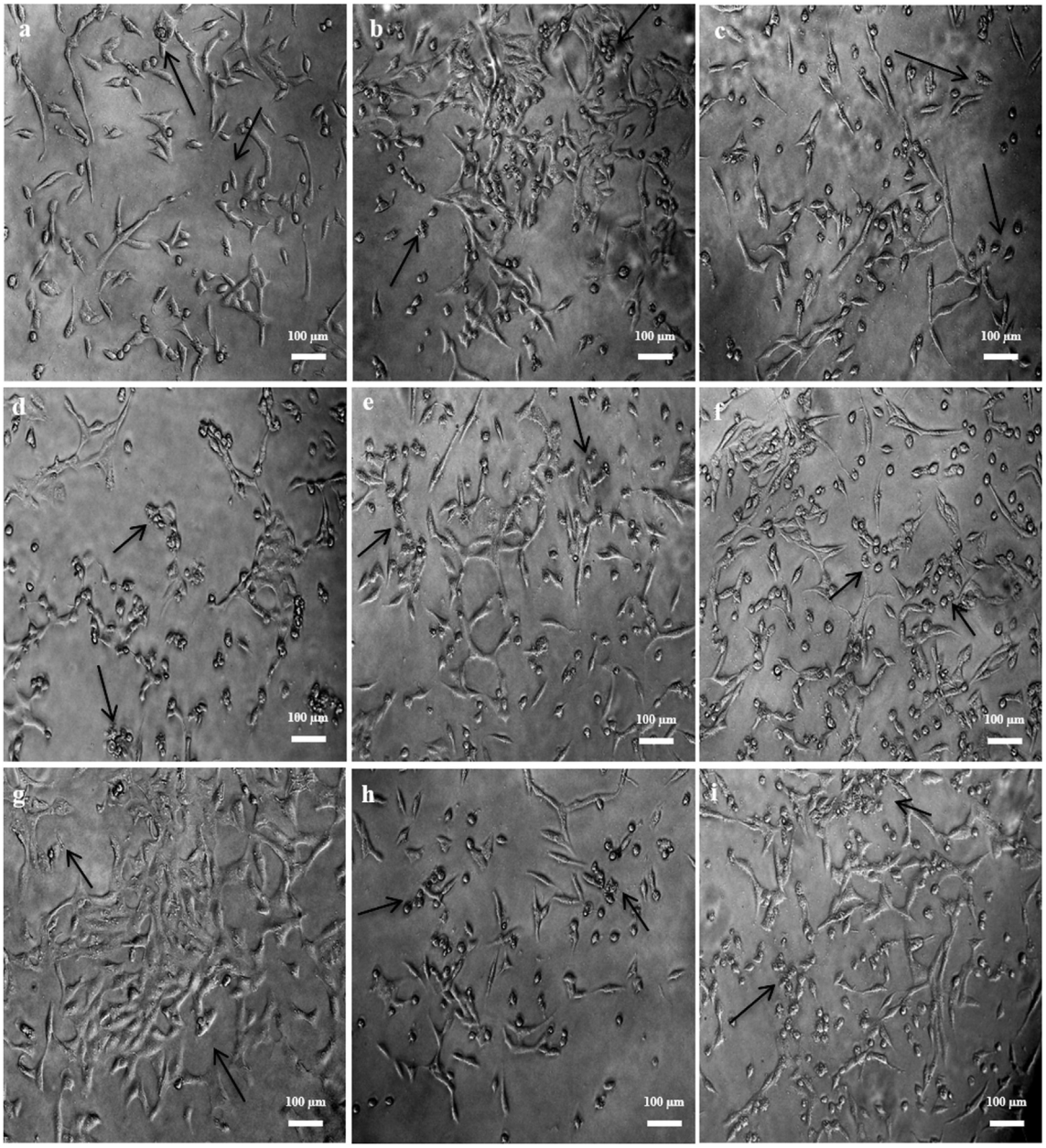

Figure 4. Morphological changes of Vero cells after 72 h co-application treatment at the IC_{50} levels for (a) AgNPs-*N. oculata*-CHL; (b) AgNPs-*T. suecica*–CHL; (c) AgNPs-*Chlorella* sp.-CHL; (d) AgNPs-*N. oculata*-ETH; (e) AgNPs-*T. suecica*-ETH; (f) AgNPs-*Chlorella* sp.-ETH; (g) AgNPs-*N. oculata*-W; (h) AgNPs-*T. suecica*-W; (i) AgNPs-*Chlorella* sp.-W, at the 5:1 ratios.

HEX and CHL; while 4,4-dimethyl-5 α-cholest-7-en-3β-ol (t_R = 31.46) of *m/z* 413.37 in MCEs-HEX. Lanosterol (t_R = 29.40) at *m/z* 425.38 was observed in MCEs-HEX, *N. oculata*-CHL and ETH, *T. suecica*-CHL and *Chlorella* sp.-MET. Fucosterol (t_R = 2.11) at *m/z* 412.65 was detected in *N. oculata* and *T. suecica*-ETH; campestanol (t_R = 20.6) and campestanol isomer (t_R = 20.93) at *m/z* 402.38 appeared in *T. suecica*-HEX and *Chlorella* sp.-CHL, HEX. Campesterol which is related to 24-methylene-ergosta-5-en-3β-ol, has only one double bond in the cyclohexane ring [45]. The 3 triterpenoids identified as 4 α-formyl-4β-methyl-5 α-cholesta-8,24-dien-3β-ol (t_R = 31.76) at *m/z* 425.34 was found in MCEs-HEX; obtusifoliol (t_R = 28.64) at 425.38 was detected in *N. oculata*-CHL, *T. suecica*-CHL, and MCEs-HEX; and squalene (t_R = 27.73) at *m/z* 410.39 was observed in *N. oculata*-CHL and HEX and *T. suecica*-CHL. Obtusifoliol acts as a common intermediate in the biosynthesis of sterols from plants and green algae [46]. Five glycolipids were tentatively identified and assigned as 1,2-dihexanoyl-sn-glycero-3-phosphoethanolamine (PE (6:0/6:0)) (t_R = 10.11) at *m/z* 411.19 detected in MCEs-HEX and CHL; 1-eicosyl-2-(9Z,12Z-heptadecadienoyl)-glycero-3-phosphate [PA (P 20:0/17:2(9Z,12Z))] (t_R = 12.89) at *m/z* 698.52 in *Chlorella* sp.-CHL, MCEs-MET and ETH; 1,2-didodecanoyl-3-(9Z-tetradecenoyl)-sn-glycerol [TG (12:0/12:0/14:1(9Z)) [iso3]] (t_R = 17.03) at *m/z* 664.56 in MCEs-MET and ETH and *N. oculata*-HEX and CHL; 1-tetradecanoyl-2-(9Z-hexadecenoyl)-glycero-3-phosphoethanolamine [PE (14:0/16:1(9Z))] (t_R = 11.32) at *m/z* 661.47 in MCEs-MET and *N. oculata* and *Chlorella* sp.-ETH; and 1-(9Z-octadecenoyl)-2-(9Z,12Z-octadecadienoyl)-sn-glycerol [DG (18:1(9Z)/18:2 (9Z,12Z)/0:0) [iso2]] (t_R = 17.84) at *m/z* 618.52 detected in *N. oculata*-CHL and *Chlorella* sp.-HEX. The positive ion mode (Table 6) identified 2 sterol lipids and 1 triterpenoid. The stoloniferone A (t_R = 32.79) was detected at *m/z* 426.32 in MCEs-CHL, MET and ETH; and 4 α-carboxy-5 α-cholesta-8,24-dien-3β-ol

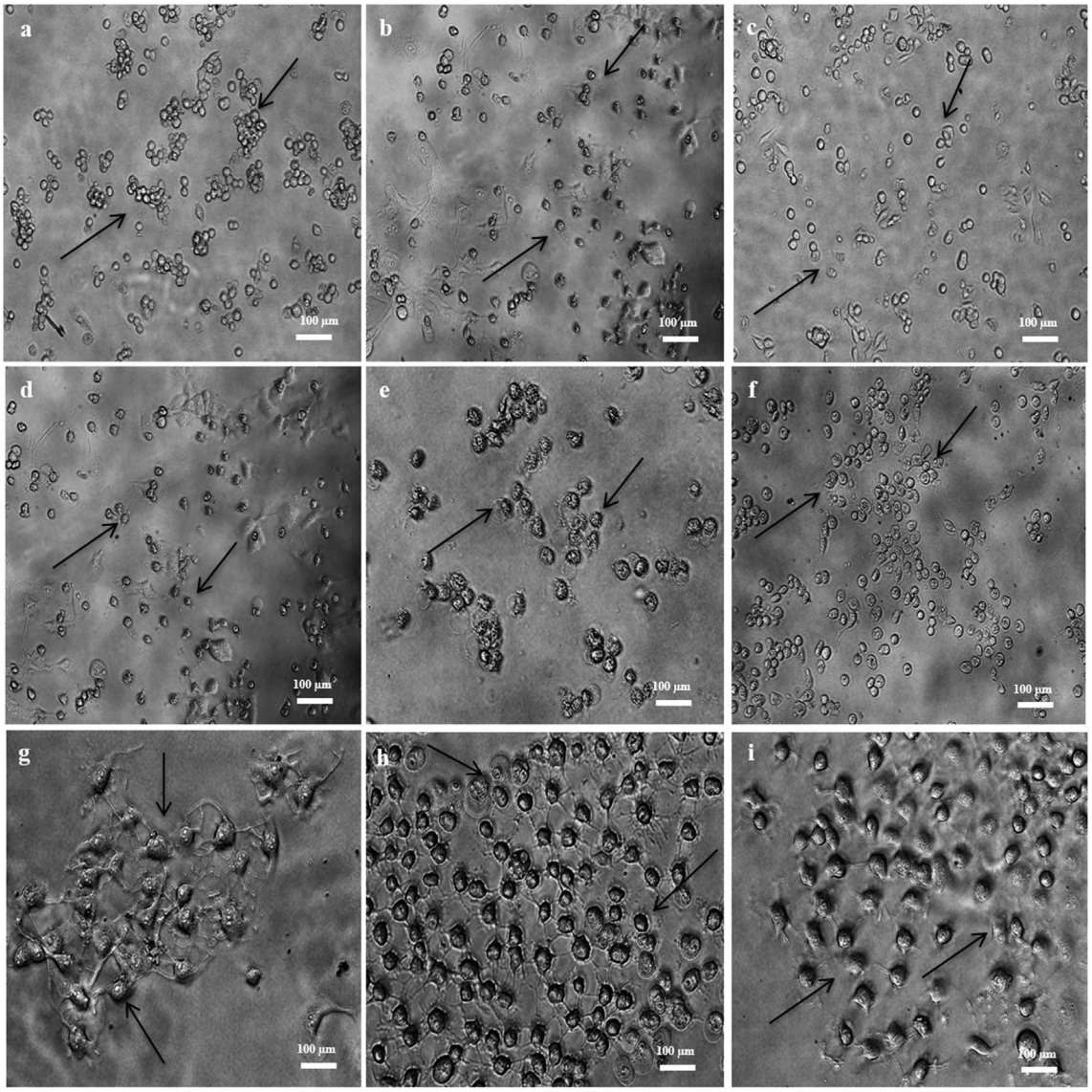

Figure 5. Morphological changes of MCF-7 cells after 72 h treatment at the IC_{50} levels for (a) AgNPs-*N. oculata*-CHL; (b) AgNPs-*T. suecica*–CHL; (c) AgNPs-*Chlorella* sp.-CHL; (d) AgNPs-*N. oculata*-ETH; (e) AgNPs-*T. suecica*-ETH; (f) AgNPs-*Chlorella* sp.-ETH; (g) AgNPs-*N. oculata*-W; (h) AgNPs-*T. suecica*-W; (i) AgNPs-*Chlorella* sp.-W, at the 5:1 ratios. The treated cells exhibited condensed nucleus in the apoptotic cells as indicated by the arrows.

(t_R = 13.56) at *m/z* 429.34 in *N. oculata*-HEX and *T. suecica*-CHL. Another triterpenoid was identified as 4 α-formyl-5 α-cholesta-8,24-dien-3β-ol (t_R = 20.45) at *m/z* 413.34 found in *N. oculata*-HEX and *Chlorella* sp.-CHL.

3.4.3. Carotenoids and chlorophylls

A total of 12 natural pigments were identified in the MCEs by the M^-H^- ion mode (Table 5). Among the carotenoids identified were apo-4′-lycopenoate at *m/z* 461.32 (t_R = 23.86) in MCEs-HEX, CHL and ETH; apo-8′-lycopenal 416.30 (t_R = 26.72) in MCEs-HEX and CHL; all-trans-β-carotene at *m/z* 536.87 (t_R = 1.4), in *T. suecica*-HEX, MET, ETH and *Chlorella* sp.-CHL, MET; 15,15′-dihydroxy-β-carotene and 15,15′-dihydroxy-β-carotene isomer (t_R = 27.82 and 28.66 min), respectively, at *m/z* 569.44, in MCEs-HEX, CHL, MET and ETH; β-carotene 15,15′ epoxide (t_R = 31.63) at *m/z* 552.88 identified in *N. oculata*-HEX, and *Chlorella* sp.-HEX, CHL, MET, ETH; and neoxanthin at *m/z* 600.88 (t_R = 16.59) identified only in *T. suecica*-HEX. The chlorophyll transformation products included protoporphyrin IX (t_R = 11.22) and protoporphyrin IX isomer (t_R = 18.44) at *m/z* 561.25, detected in MCEs-ETH and as the isomer in MCEs-MET and *Chlorella* sp.-ETH; coproporphyrinogen I and coproporphyrinogen I isomer exhibiting the characteristic peak at *m/z* 659.31 with t_R = 15.80 and t_R = 24.80, respectively, observed in *N. oculata*-CHL, ETH, *Chlorella* sp.-CHL; *N. oculata* and *Chlorella* sp.-CHL and MCEs-ETH.

For positive ions, Table 4 shows the presence of meso-Zeaxanthin/(3R,3′S)-Zeaxanthin (t_R = 26.48) in *N. oculata*-W and *T. suecica*-W; and the isomer (t_R = 32.91) at *m/z* 569.44 detected in MCEs-W; methyl pyropheophorbide (t_R = 1.71) at *m/z* 548.67 detected only in MCEs-W; protoporphyrinogen IX (t_R = 20.03) which appeared in *N. oculata*-W and *T. suecica*-W, and protoporphyrinogen IX isomer (t_R = 28.32) at *m/z* 591.29 in MCEs-W. For carotenoids, apo-4′-lycopenoate (t_R = 29.60) was detected in *N. oculata*-HEX, *Chlorella* sp.-CHL and apo-4′-lycopenoate isomer (t_R = 29.84) at *m/z* 499.36 in *N. oculata*-HEX, *T. suecica*-MET, and *Chlorella* sp.-MET, CHL; all-trans-β-carotene (t_R = 1.46) in MCEs-HEX, CHL, ETH, and all-trans-β-carotene isomer (t_R = 2.06) at *m/z* 536.89 in MCEs- CHL, HEX, and *T. suecica*, *Chlorella* sp.-ETH. The MCEs-MET, *T. suecica*-HEX, ETH and *Chlorella* sp.-HEX extracts contained 15,15′-dihydroxy-&β-carotene (t_R = 1.42) at *m/z* 570.89; and meso-zeaxanthin/(3R,3′S)-zeaxanthin (t_R = 26.48) was detected in *Chlorella* sp.-MET, ETH, and its isomer (t_R = 32.91) at *m/z* 569.44 in *N. oculata*-HEX, CHL, MET, *T. suecica*-HEX, CHL, MET, ETH, and *Chlorella* sp.-ETH. α-cryptoxanthin (t_R

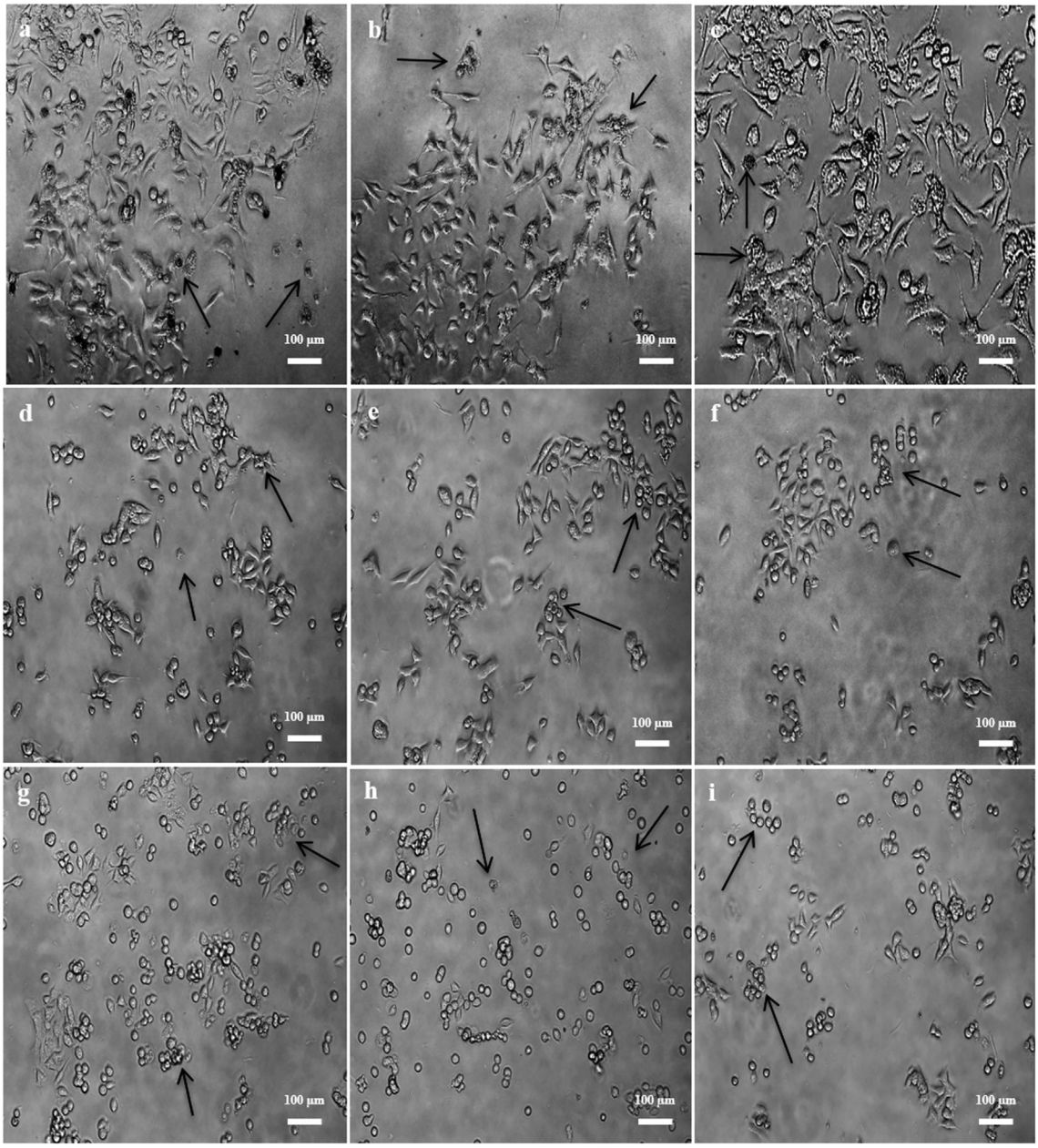

Figure 6. Morphological changes of 4T1 cells after 72 h co-application treatment at the IC_{50} levels for (a) AgNPs-*N. oculata*-CHL; (b) AgNPs-*T. suecica*–CHL; (c) AgNPs-*Chlorella* sp.-CHL; (d) AgNPs-*N. oculata*-ETH; (e) AgNPs-*T. suecica*-ETH; (f) AgNPs-*Chlorella* sp.-ETH; (g) AgNPs-*N. oculata*-W; (h) AgNPs-*T. suecica*-W; (i) AgNPs-*Chlorella* sp.-W, at the 5:1 ratios.

= 14.55) at *m/z* 553.41 was found only in *N. oculata*-CHL. Violaxanthin, which has been reported to exhibit strong anti-proliferative effect on MCF-7 cells, and induce biochemical changes associated with early apoptosis, was detected in MCEs-MET, *N. oculata*-ETH, *Chlorella* sp.-ETH. Violaxanthin and the derivatives obtained through pharmacomodulation should be studied as new possible drugs for the treatment of breast cancer [47]. Fucoxanthin at *m/z* 658.90 (t_R = 1.63), was observed in MCEs-CHL and ETH. Anti-proliferative and anticancer effects of fucoxanthin and fucoxanthinol interact through various signaling pathways including the Bcl-2 proteins, caspases, PI3K/Akt, MAPK, JAK/STAT, GADD45, AP-1, and many other molecules involved in the cell cycle arrest, apoptosis, anti-angiogenesis or malignant tumor inhibition [48]. Lutein (t_R = 1.44) and lutein isomer (t_R = 1.89) showed protonated ions at *m/z* 568.87, and were detected in MCEs-MET, ETH, *T. suecica*-HEX, and in MCEs-HEX, CHL, MET, ETH, respectively; neoxanthin (t_R = 1.67) at *m/z* 600.89, was found only in *N. oculata*-HEX and *Chlorella* sp.-CHL. Other carotenoids could not be positively identified due to inadequate ionization [49]. Chlorophyll transformation products including protoporphyrin IX (t_R = 14.14), protoporphyrin IX isomer (t_R = 16.37) and protoporphyrin IX isomer (t_R = 17.52) at *m/z* 563.26, were observed in MCEs-MET, *N. oculata, T. suecica*-ETH; MCEs-MET, ETH; and MCEs-ETH, respectively. Protoporphyrinogen IX (t_R = 20.03) at *m/z* 591.29 appeared in *T. suecica*-CHL.

3.4.4. Fatty amides, amino acids and vitamins

The fatty amides (Table 5) were identified as N-palmitoyl phenylalanine (t_R = 11.08) and N-palmitoyl phenylalanine isomer (t_R = 15.81) based on *m/z* 403.31, which were detected in MCEs-CHL; all trans-retinyl palmitate (t_R = 23.38) and all trans-retinyl palmitate isomer (t_R = 24.66) with the characteristic peaks at *m/z* 523.45, were observed in *N. oculata* HEX, CHL, ETH, *Chlorella* sp.-MET, and *N. oculata*-HEX, *T. suecica*-CHL, respectively; N-oleoyl glutamine (t_R = 13.68) and N-oleoyl glutamine

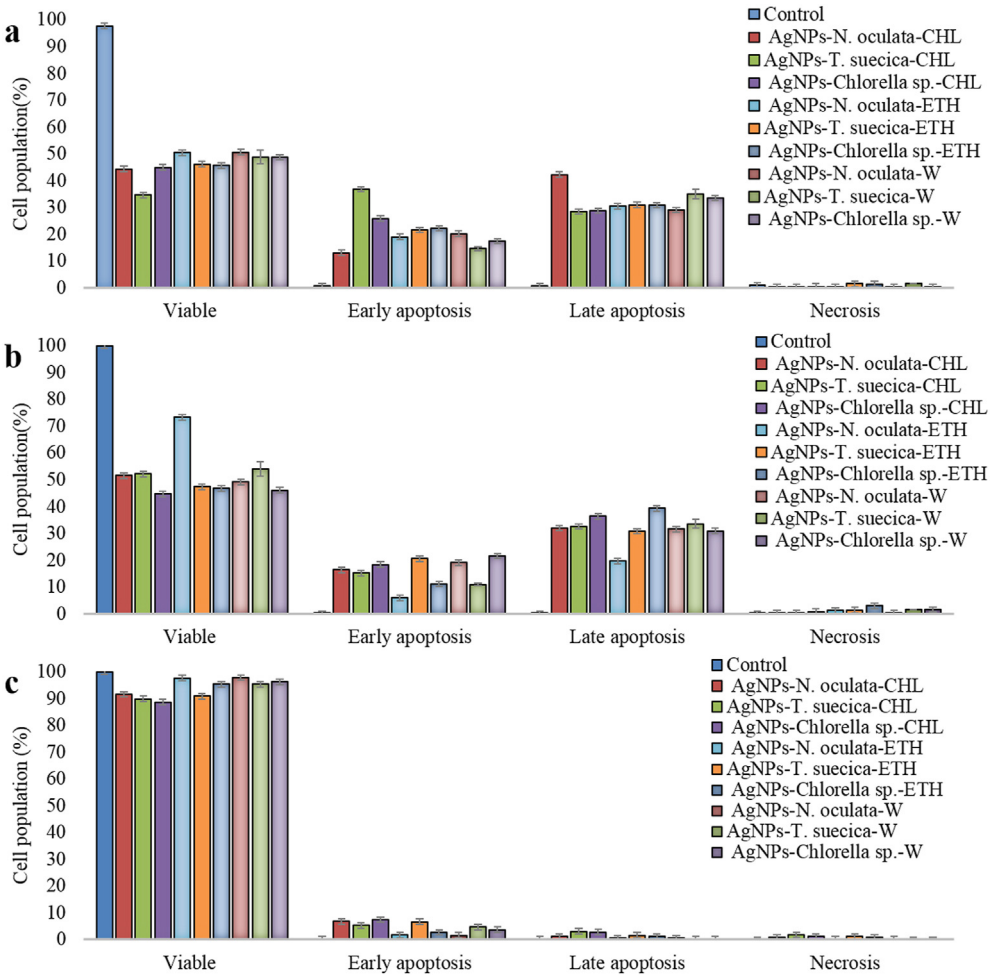

Figure 7. Flow cytometric analysis after 24 h treatment of AgNPs-MCEs-CHL and AgNPs-MCEs-W and ETH at the 5:1 ratios, on (a) MCF-7; (b) 4T1; (c) Vero cell-lines. Control represents the untreated cells. The viable (Annexin V^-PI^-), early apoptotic (Annexin V^+PI^-), late apoptotic (Annexin V^+PI^+), and necrotic (Annexin V^-PI^+) cells were based on the staining ($^+$ stained; $^-$ not stained). All values are expressed as Mean ± SE.

isomer (t_R = 27.76) at *m/z* 410.31, were determined in all MCEs, and MCEs-CHL, *N. oculata*-HEX, respectively. Amino acids assigned as geranylgeranylcysteine (t_R = 1.64) was found in all MCEs, and geranylgeranylcysteine isomer (t_R = 1.92) was found in MCEs-W (Table 4), CHL, MET, ETH and *T. suecica*-HEX at *m/z* 407.24. Four vitamins were identified including phylloquinone (t_R = 1.59) at *m/z* 450.77, detected in MCEs-W (Table 4), CHL, MET, ETH and *T. suecica*-HEX. The phylloquinones known as vitamin K1 has been isolated from plants and algae [50]. Thiamin triphosphate (t_R = 14.45) at *m/z* 504.25, was found abundant in MCEs-CHL. Ascorbyl palmitate (t_R = 32.24) and ascorbyl palmitate isomer (peak 42) (t_R = 33.13) were detected in MCEs-HEX, CHL, showing the characteristic peak at *m/z* 414.26.

For positive ion mode, 3 fatty amides, 1 amino acid and 12 vitamins were identified (Table 6). Termitomycamide B (t_R = 16.11), termitomycamide B isomer (t_R = 20.60) and termitomycamide B isomer (t_R = 29) were detected at *m/z* 436.30, were found in *T. suecica*-MET, ETH; *N.* oculata-MET, *T. suecica*-MET, ETH, *Chlorella* sp.-ETH; and MCEs-MET, ETH, *T. suecica*-HEX, *Chlorella* sp.-HEX, CHL extracts, respectively. N-arachidonoyl glutamic acid (t_R = 14.76) was determined in *T. suecica*-MET, ETH and *Chlorella* sp.-MET at *m/z* 433.28. Phylloquinone (t_R = 1.74) at *m/z* 450.73 was only detected in MCEs-W. Riboflavin cyclic-4′,5′-phosphate (t_R = 18.20) was identified at *m/z* 438.32 in *N. oculata*-W, *T. suecica*-MET and *Chlorella* sp.-ETH. β-tocopherol, β-tocopherol isomer and β-tocopherol isomer were determined at *m/z* 416.37 with t_R = 11.89, 12.71, and 13.73, respectively, and observed in *Chlorella* sp.-W; *T. suecica*-HEX; and MCEs-MET, ETH, respectively. Ascorbyl palmitate was shown at *m/z* 415.2638 and t_R = 13.58 in *N. oculata*-HEX, while ascorbyl stearate (t_R = 28.17) and ascorbyl stearate isomer (t_R = 29.07) at *m/z* 442.30 were detected only in *N. oculata* and *T. suecica*-W (Table 4).

3.4.5. Other compounds

The metabolites identified in negative ion mode included 3 flavones, 2 flavonoids and 1 prenylated chalcone. Qancaonin Q (t_R = 15.11) and gancaonin Q isomer (t_R = 15.32) assigned at *m/z* 406.17, were found in *N. oculata*-W, CHL, *T. suecica*-HEX, *Chlorella* sp.-W, HEX, ETH; and MCEs-W, HEX, ETH, *Chlorella sp.*-CHL, *T. suecica*-MET, respectively. Prenylated chalcone (Paratocarpin E) (t_R = 15.27) was identified at *m/z* 408.21, found in MCEs-CHL and *N. oculata*, *T. suecica*-W (Tables 4 and 5). Paratocarpin E has shown significant anti-cancer effects on human cancer cell-lines and stimulated both autophagy and apoptosis in MCF-7 cells [51]. Two phenols were detected and characterized as 2-methoxy-6-(all--trans-heptaprenyl) phenol (t_R = 25.78) and 2-methoxy-6-(all-trans-heptaprenyl) phenol isomer (t_R = 26.61) at *m/z* 599.48, observed in MCEs-CHL, MET, ETH; and MCEs-CHL, *N. oculata, Chlorella* sp.-MET, ETH extracts, respectively. Three glucose metabolites were identified (Table 5) - UDP- α-D-glucose (t_R = 15.11) at *m/z* 566.30 in *N. oculata*-ETH, *T. suecica*-MET and *Chlorella* sp.-MET, ETH; and D-glucosyl-sphingosine (t_R = 18.48) and D-glucosyl-sphingosine isomer (t_R = 20.71) at *m/z* 461.65 identified in MCEs-CHL and *N. oculata*-CHL, respectively. 8-oxo-dGDP (t_R = 10.76) and 8-oxo-dADP (t_R = 10.98) were tentatively identified at *m/z* 443.21 and 424.18, respectively, detected in MCEs-W, CHL, ETH, *N. oculata*-MET, *Chlorella* sp.-MET; and MCEs-CHL, MET, ETH, W. The

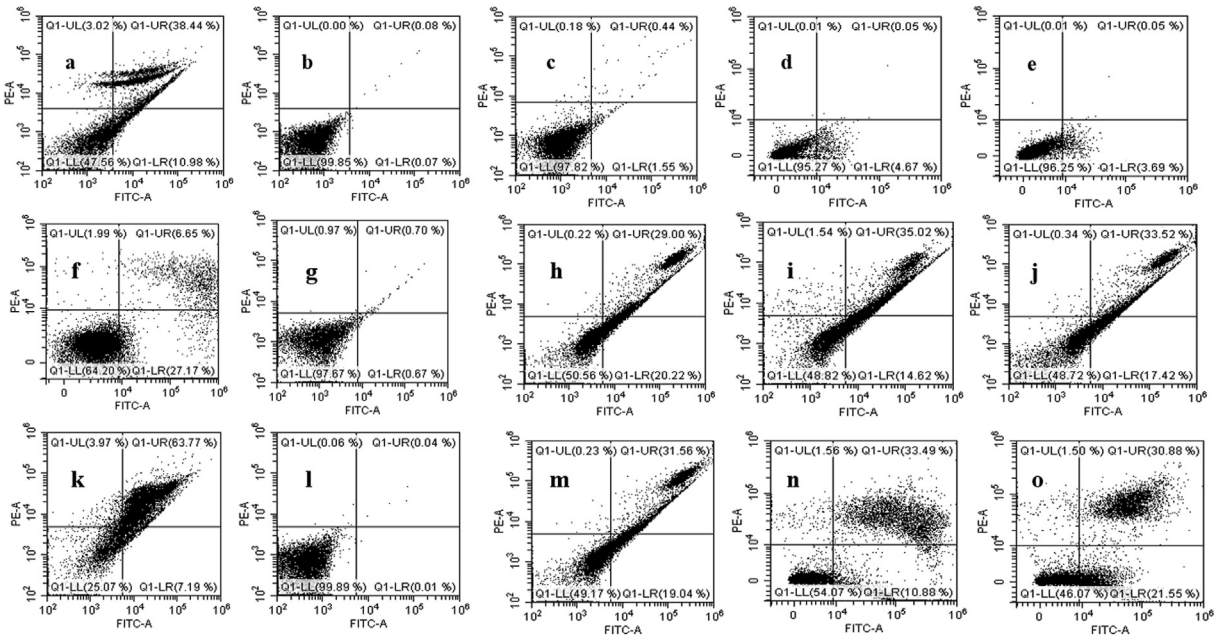

Figure 8. Flow cytometric analyses after 24 h treatment on i- Vero cells from (a) Positive control; (b) Negative control; (c) AgNPs-*N. oculata*-W; (d) AgNPs-*T. suecica*-W; (e) AgNPs-*Chlorella* sp.-W; ii- MCF-7 cells from (f) Positive control; (g) Negative control; (h) AgNPs-*N. oculata*-W; (i) AgNPs-*T. suecica*-W; (j) AgNPs-*Chlorella* sp.-W; iii- 4T1 cells from (k) Positive control; (l) Negative control; (m) AgNPs-*N. oculata*-W; (n) AgNPs-*T. suecica*-W; (o) AgNPs-*Chlorella* sp.-W (Positive control: Tamoxifen treatment; Negative control: Untreated cells; All co-applications at the 5:1 ratios).

2-(α-hydroxyethyl) thiamine diphosphate (t_R = 10.43) and 2-α-hydroxyethyl) thiamine diphosphate isomer (t_R = 26.81) were determined at *m/z* 468.06 in MCEs-CHL and *N. oculata*-CHL, respectively. Geranylgeranyl diphosphate (GGPP) is one of the key isoprenoids to be converted into compounds necessary for plant growth such as gibberellins, carotenoids, chlorophylls, isoprenoid quinones, and geranylgeranylated small G proteins such as Rho, Rac, and Rab [52]. GGPP (t_R = 22.90) and GGPP isomer (t_R = 32.93) were found at *m/z* 450.45 in MCEs HEX, *N. oculata*-CHL, W, ETH, *T. suecica*-W, *Chlorella* sp.-CHL, MET; and MCEs-CHL, *N. oculata*-HEX, MET, *Chlorella* sp.-MET, ETH, respectively. The metabolite tentatively identified as didecyl phthalate at *m/z* 446.73 (t_R = 1.81 min) was found in MCEs-W and *T. suecica*-ETH. This belongs to benzoic acid esters, derived from the oxidation of fatty acids and has been reported in marine organisms. Three leukotrienes were identified - leukotriene-D4 (t_R = 17.31), leukotriene-C4 isomer (t_R = 19.94) and leukotriene-C4 isomer (t_R = 40.41) were determined at *m/z* 496.66 and

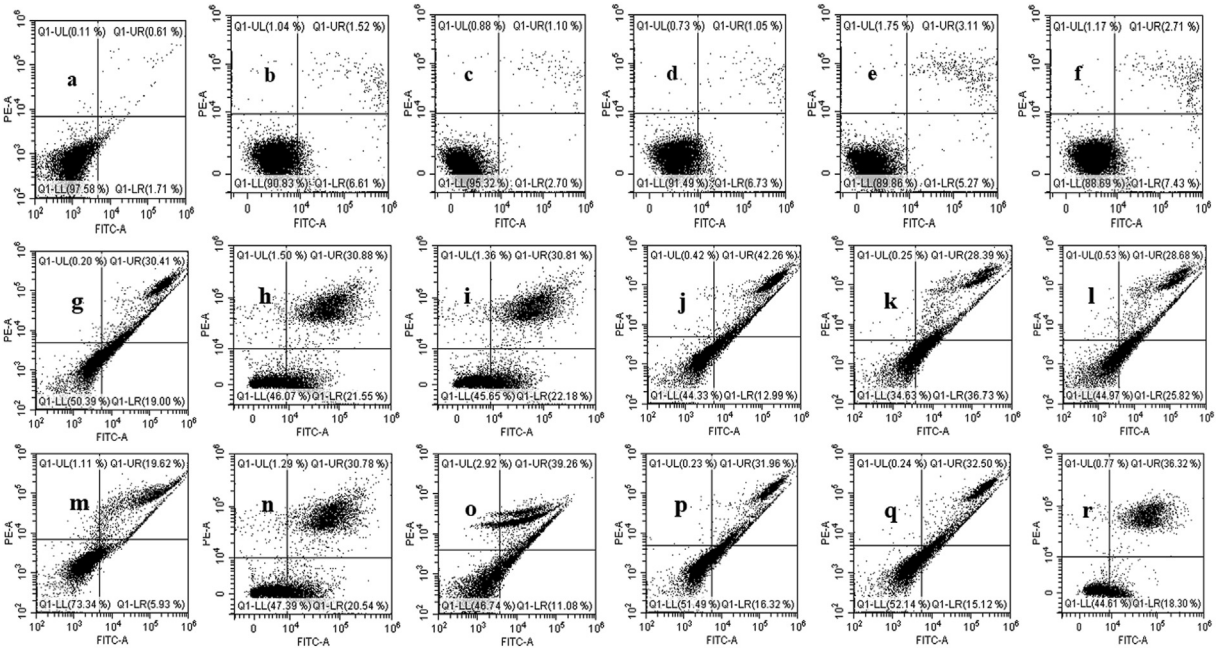

Figure 9. Flow cytometric analyses after 24 h treatment at the 5:1 ratios on i- Vero cells from (a) AgNPs-*N. oculata*-ETH; (b) AgNPs-*T. suecica*-ETH; (c) AgNPs-*Chlorella* sp.-ETH; (d) AgNPs-*N. oculata*-CHL; (e) AgNPs-*T. suecica*–CHL; (f) AgNPs-*Chlorella* sp.-CHL; ii- MCF-7 cells from (g) AgNPs-*N. oculata*-ETH; (h) AgNPs-*T. suecica*-ETH; (i) AgNPs-*Chlorella* sp.-ETH; (j) AgNPs-*N. oculata*-CHL; (k) AgNPs-*T. suecica*–CHL; (l) AgNPs-*Chlorella* sp.-CHL; iii- 4T1 cells from (m) AgNPs-*N. oculata*-ETH; (n) AgNPs-*T. suecica*-ETH; (o) AgNPs-*Chlorella* sp.-ETH; (p) AgNPs-*N. oculata*-CHL; (q) AgNPs-*T. suecica*–CHL; (r) AgNPs-*Chlorella* sp.-CHL.

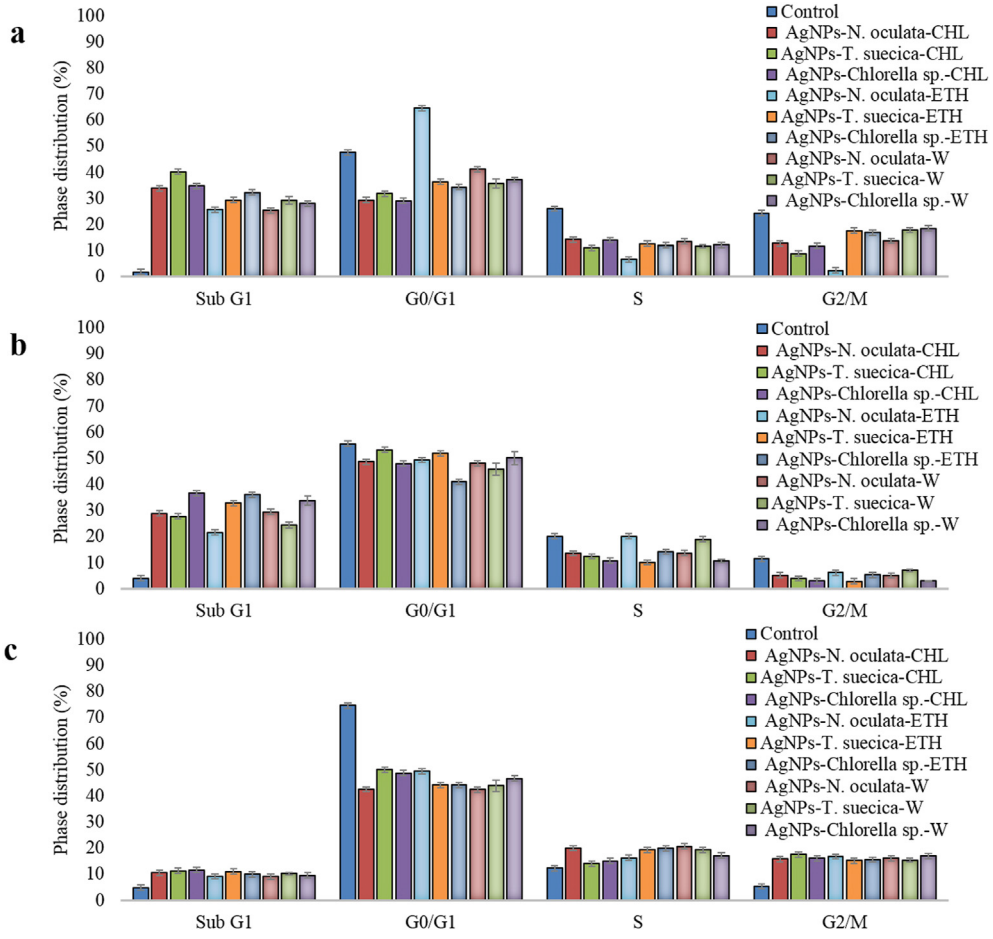

Figure 10. Composition of sub-G1, G1, S and G2/M phase after 24 h treatment of AgNPs-MCEs-CHL and AgNPs-MCEs-W and ETH at the 5:1 ratios on (a) MCF-7; (b) 4T1; (c) Vero cell line. Control represents the untreated cells. Each figure is representative of three independent experiments ($n = 3$) and the results are statistically significant ($p < 0.05$).

625.30. These were found in *N. oculata*-HEX, ETH, *T. suecica*-ETH; MCEs-MET, ETH, *T. suecica*-CHL; and MCEs MET, ETH, *Chlorella* sp.-CHL, respectively. Two alkanes were identified as hexatriacontane (t_R = 32.68) and hexatriacontane isomer (t_R = 33.14) at *m/z* 506.978, in *T. suecica*-MET; and *T. suecica*-MET, *N. oculata,* ETH, respectively. A heptasiloxane, hexadecamethyl- (t_R = 12.05), was determined at *m/z* 533.0748 in MCEs-MET, *N. oculata*-CHL, ETH, *T. suecica*-ETH, and *Chlorella* sp.-CHL. The unknown (t_R = 15.37) was identified at *m/z* 435.27, found in all MCEs.

For positive ion mode, five metabolites were identified as flavonoids (Table 6). Quercetin 3-(2″ galloylrhamnoside) (t_R = 17.25) and quercetin 3-(2″-galloylrhamnoside) isomer (t_R = 26.83) at *m/z* 600.11 were detected in *Chlorella* sp.-MET and *N. oculata*-CHL, respectively; quercetin 7-methyl ether 3,3′,4′-trisulfate (t_R = 20.95) was identified at *m/z* 555.93 in *T. suecica*-MET, ETH and *Chlorella* sp.-MET. The positive ion at *m/z* 406.22 suggests the presence of erycristin (t_R = 23.68) in MCEs-CHL, ETH and *N. oculata*-MET, *Chlorella* sp.-MET. Kolaflavanone (t_R = 14.67) at *m/z* 588.23 was observed in *N. oculata, T. suecica*-ETH and *Chlorella* sp.-MET. Three glucose metabolites were identified as stachyose (t_R = 1.82) at *m/z* 666.56 in MCEs-W (Table 4); dTDP- α-D-glucose (t_R = 12.15) at *m/z* 564.33 in MCEs-ETH, *N. oculata*-MET, *T. suecica*-MET; and Cucurbitacin I 2-glucoside at *m/z* 676.37 (t_R = 9.77) detected in MCEs-MET, ETH. Organic compound known as pyrimidine 2′-deoxyribonucleoside diphosphates (peak 48) identified as dUDP (t_R = 1.6 min) at *m/z* 404.16 was found in *N. oculata*-ETH and *Chlorella* sp.-MET. Phytanoyl CoA, a coenzyme A derived from phytanic acid, found in human food or animal tissues, can be derived from chlorophyll in the plant extracts. It is an epimeric metabolite for the side chain of the chlorophyll [53], identified at *m/z* 531.71 (t_R = 9.41 min) in MCEs-MET, *N. oculata*-CHL, ETH, *Chlorella* sp.-CHL, ETH. Presqualene diphosphate is a triterpenyl phosphate or a presqualene in which the hydroxyl hydrogen is replaced by a diphosphate group. It is an intermediate in the biosynthesis of terpenoid [53], identified at *m/z* 586.71 (t_R = 28.96 min) in *Chlorella* sp.-ETH. Four alkane were tentatively identified (Tables 4 and 6) as tetracontane (t_R = 12.17), tetracontane isomer (t_R = 19.59) and tetracontane isomer (t_R = 28.32) at *m/z* 563.08, found in *N. oculata*-MET, ETH, *Chlorella* sp.-MET; *Chlorella* sp.-MET; and *Chlorella* sp.-HEX extracts, respectively; and hexatriacontane at *m/z* 506.97 (t_R = 27.95 min) in *N. oculata*-W. Canthiumine (t_R = 16.81) at *m/z* 552.27 is a cyclic peptide detected in MCEs-MET and ETH. Didecyl phthalate (t_R = 1.81) at *m/z* 446.7300 was tentatively identified in MCEs-W. Heptasiloxane, hexadecamethyl- (t_R = 15.91) and heptasiloxane, hexadecamethyl-isomer (t_R = 19) were identified at *m/z* 533.14, in *N. oculata*-W, *T. suecica*-ETH, *Chlorella* sp.- ETH; and *N. oculata*-W, respectively. Other ions were observed but the obtained MS data did not allow their complete identification (unknown compounds).

4. Discussion

Antitumor activity of microalgal compounds has been attributed to their lipophilicity that can cross the membranes and interact with proteins involved in apoptosis. The compounds could stimulate DNA-dependent DNA polymerase inhibition, alter cyclins expression or most of the transduction pathway, trigger immune response [54], and also

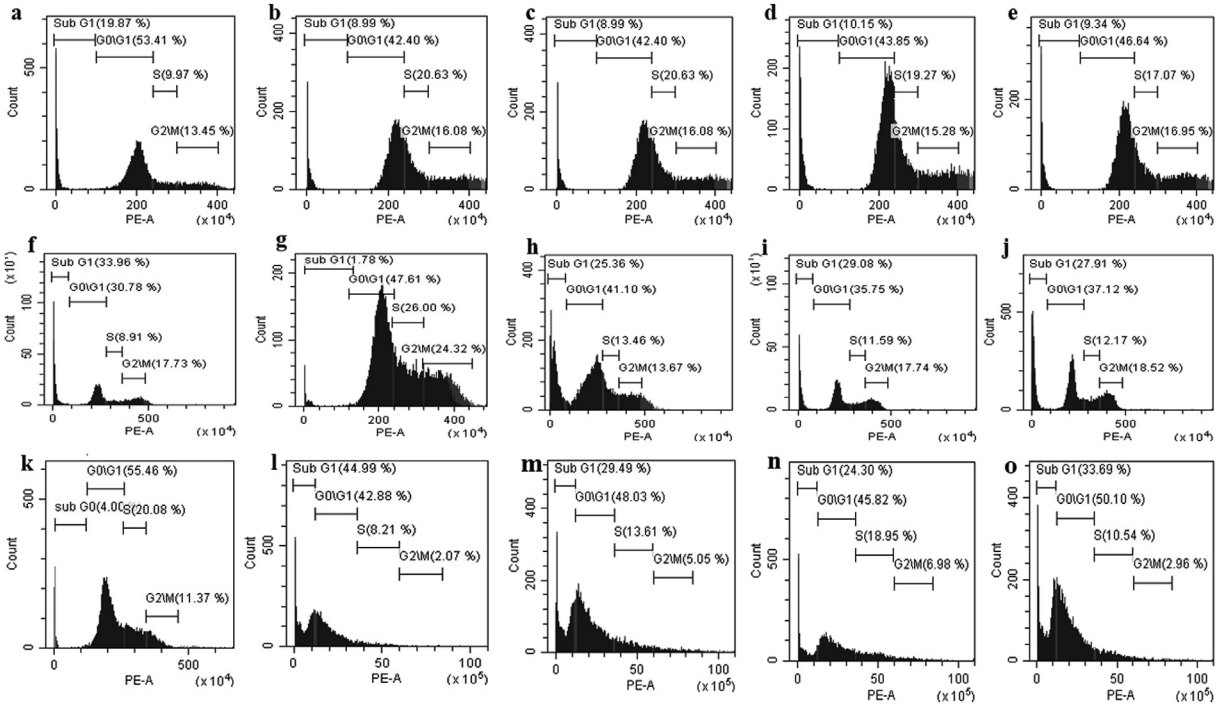

Figure 11. Cell cycle analysis after 24 h treatment for on i- Vero cells from (a) Positive control; (b) Negative control; (c) AgNPs-*N. oculata*-W; (d) AgNPs-*T. suecica*-W; (e) AgNPs-*Chlorella* sp.-W; ii- MCF-7 cells from (f) Positive control; (g) Negative control; (h) AgNPs-*N. oculata*-W; (i) AgNPs-*T. suecica*-W; (j) AgNPs-*Chlorella* sp.-W; iii- 4T1 cells from (k) Positive control; (l) Negative control; (m) AgNPs-*N. oculata*-W; (n) AgNPs-*T. suecica*-W; (o) AgNPs-*Chlorella* sp.-W (Positive control: Tamoxifen treatment; Negative control: Untreated cells; All co-applications at the 5:1 ratios).

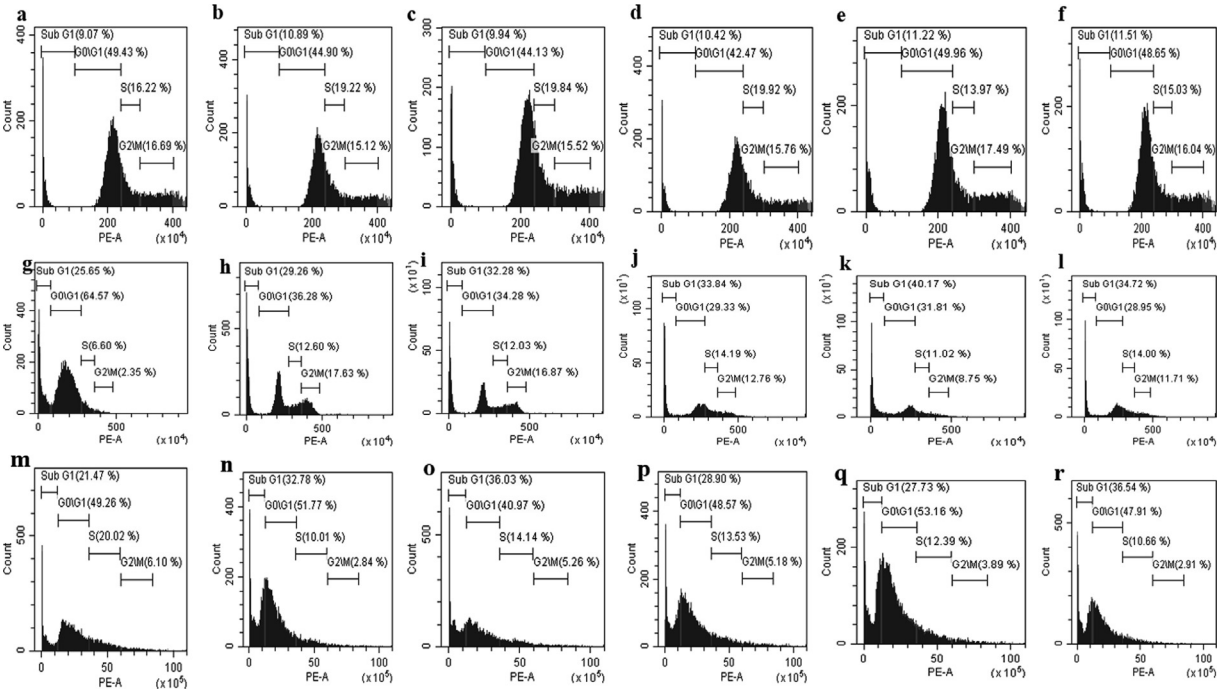

Figure 12. Cell cycle analyses after 24 h treatment at the 5:1 ratios on i- Vero cells from (a) AgNPs-*N. oculata*-ETH; (b) AgNPs-*T. suecica*-ETH; (c) AgNPs-*Chlorella* sp.-ETH; (d) AgNPs-*N. oculata*-CHL; (e) AgNPs-*T. suecica*–CHL; (f) AgNPs-*Chlorella* sp.-CHL; ii- MCF-7 cells from (g) AgNPs-*N. oculata*-ETH; (h) AgNPs-*T. suecica*-ETH; (i) AgNPs-*Chlorella* sp.-ETH; (j) AgNPs-*N. oculata*-CHL; (k) AgNPs-*T. suecica*–CHL; (l) AgNPs-*Chlorella* sp.-CHL; iii- 4T1 cells from (m) AgNPs-*N. oculata*-ETH; (n) AgNPs-*T. suecica*-ETH; (o) AgNPs-*Chlorella* sp.-ETH; (p) AgNPs-*N. oculata*-CHL; (q) AgNPs-*T. suecica*–CHL; (r) AgNPs-*Chlorella* sp.-CHL.

induce cytotoxicity against different cancer cell-lines [55, 56]. The mechanisms for AgNPs-induced cytotoxicity on the cancer cells are attributable to the oxidative stress, mitochondrial damage, induction of apoptosis and DNA damage [57]. The biogenic AgNPs have been proposed as the adjuvant for the antibiotic activities in the treatment of infectious diseases caused by the bacteria [58]. The mechanisms involve the bonding reaction between the NPs and the bioactive molecules in which the hydroxy and amino groups can interact with the large surface

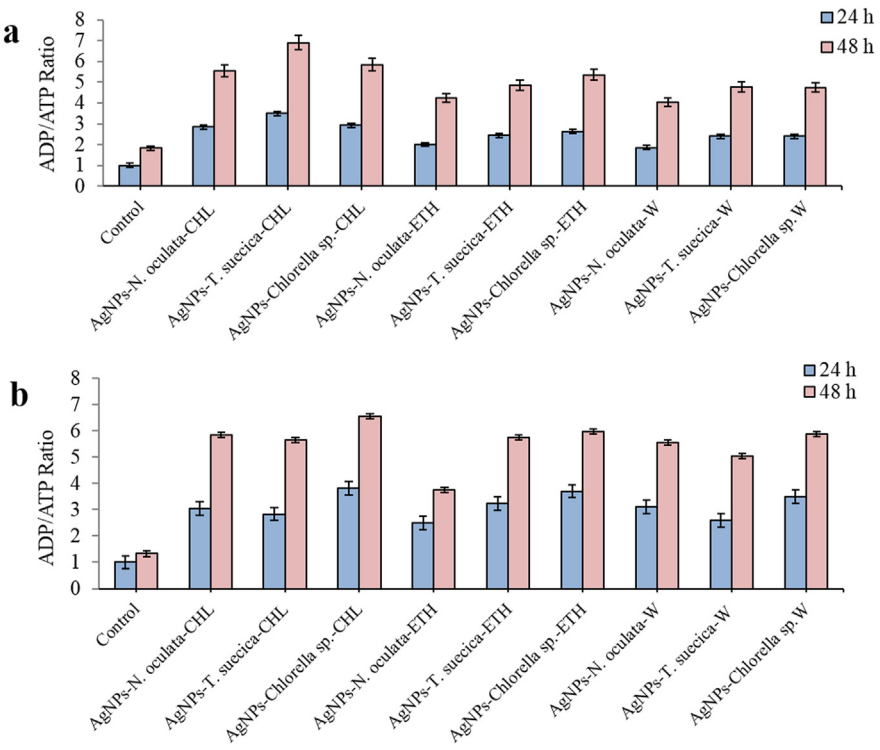

Figure 13. Effects of AgNPs-MCEs-CHL and AgNPs-MCEs-W and ETH at the IC_{50} levels after 24 and 48 h treatments on ADP/ATP ratio of (a) MCF-7; (b) 4T1 cell line (Control represents the untreated cells; All co-applications at the 5:1 ratios). All values are expressed as Mean ± SE.

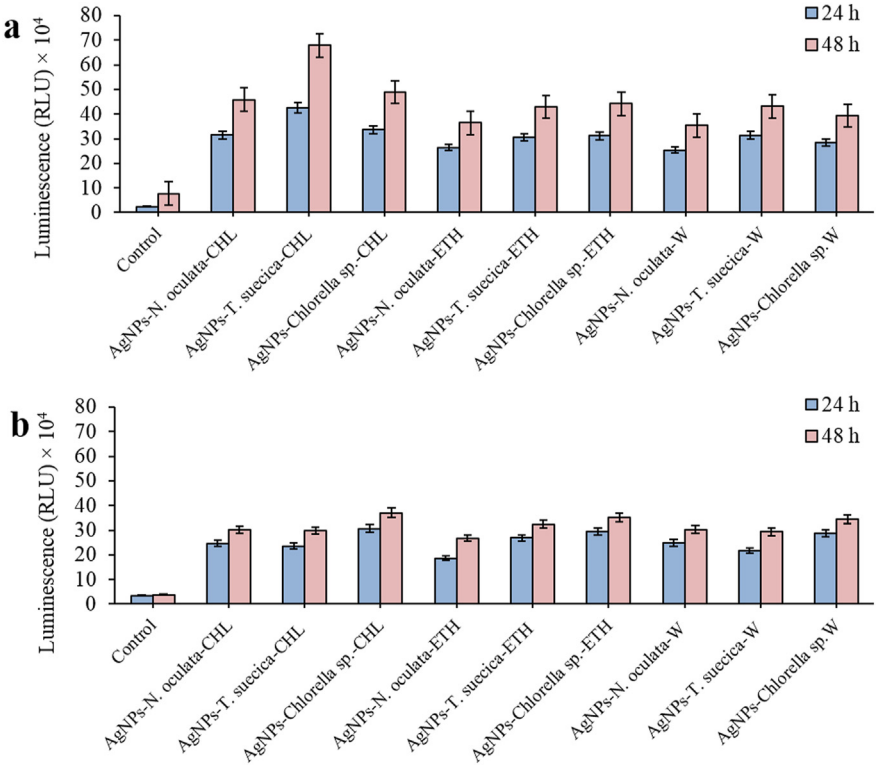

Figure 14. Effects of AgNPs-MCEs-CHL and AgNPs-MCEs-W and ETH at the IC_{50} levels after 24 and 48 h treatments on the Caspase 3/7 activities analyzed using Caspase-Glo® 3/7 assay of (a) MCF-7; (b) 4T1 cell line (Control represents the untreated cells; All co-applications at the 5:1 ratios). All values are expressed as Mean ± SE.

Table 4. Metabolites identification from MCEs-W by using LC-ESI-MS negative [M-H(-)] and positive ionization mode [M+H(+)] (The symbol "+" indicates "Present", and "ND "indicates "Not detected").

Compounds	t_R	m/z	*N. oculata*	*T. suecica*	*Chlorella sp*
Negative Ions					
1. Fatty acid					
Stearidonoyl-CoA	1.39	544.94	+	+	+
Octadecanoic acid trichloroethyl ester isomer	32.08	414.18	+	+	+
2. Fatty amides					
N-oleoyl glutamine	13.68	410.31	+	+	+
3. Amino acid					
Geranylgeranylcysteine	1.64	407.24	+	+	+
Geranylgeranylcysteine isomer	1.92	407.24	+	+	+
4. Vitamins					
Phylloquinone	1.59	450.77	+	+	+
5. Others					
Gancaonin Q	15.11	406.17	+	ND	+
Gancaonin Q isomer	15.32	406.17	+	+	+
Paratocarpin E	15.27	408.21	+	+	ND
8-oxo-dGDP	10.76	443.21	+	+	+
8-oxo-dADP	10.98	424.18	+	+	+
Geranylgeranyl diphosphate	22.90	450.45	+	+	ND
Didecyl phthalate	1.81	446.73	+	+	+
Unknown	15.37	435.27	+	+	+
Positive Ions					
1. Carotenoids					
Meso-Zeaxanthin/(3R,3′S)-Zeaxanthin	26.48	569.44	+	+	ND
Meso-Zeaxanthin/(3R,3′S)-Zeaxanthin isomer	32.91	569.44	+	+	+
2. Chlorophyll					
Methyl pyrophaeophoribide	1.71	548.67	+	+	+
Protoporphyrinogen IX	20.03	591.29	+	+	ND
Protoporphyrinogen IX isomer	28.32	591.29	+	+	+
3. Vitamins					
Riboflavin cyclic-4′,5′-phosphate	18.20	438.32	+	ND	ND
Phylloquinone	1.59	450.77	+	+	+
Ascorbyl stearate	28.17	442.30	+	+	ND
Ascorbyl stearate isomer	29.07	442.30	+	+	ND
4. Others					
Stachyose	1.82	666.56	+	+	+
Hexatriacontane	27.95	506.97	+	ND	ND
Didecyl phthalate	1.79	446.68	+	+	ND
Heptasiloxane, hexadecamethyl-	15.91	533.14	+	ND	ND
Heptasiloxane, hexadecamethyl- isomer	19	533.14	+	ND	ND

area of the AgNPs *via* chelation [59]. The AgNPs may damage the cell metabolism, disulfide bond formation, and iron homeostasis, resulting in cell death [60]. This may also increase the production of reactive oxygen species (ROS) and membrane permeability to induce the activity of a wide range of bioactive molecules. In the case of gram-negative bacteria, the antibiotic activity in several metabolic states may be promoted, or the antibiotic ability towards a resistant bacterial strain may be restored [59].

The type of solvent and extraction procedures could affect the composition and biological effects of the extracts [61]. The major advantage of AgNPs-MCEs–W, ETH is the use of water and ethanol as green solvents to produce the MCEs. CHL is not environmentally-friendly and also toxic. Both ETH and W, on the other hand have low toxicity as compared to the other organic solvents [62]. ETH is known as a good solvent for polyphenol extraction and safe for human consumption [63]. The W extracts may have more non-phenolic compounds or contain phenolic compounds that have a smaller amount of active groups than the other solvents [64]. In successive extraction, this can be complementary. The *Padina gymnospora* water extracts show high inhibition of lipid oxidation in the liposomes, while the ethanol extracts show a pro-oxidative activity. Although the water extracts have less phenolic content and low radical scavenging activity as compared to the ethanolic extracts, the iron chelating activity is reportedly high [65]. The highest cytotoxicity of AgNPs-MCEs–W, ETH on the breast cancer can be correlated to the increased early and late apoptotic events, increased sub G1 (apoptotic events) with enhanced biomarker activities. The incorporation of the MCEs in the AgNPs-MCEs–W, ETH formulation, using water or ethanol as extracting solvent, was proven effective to reduce the cytotoxicity of the AgNPs on the non-cancerous healthy cells. This could potentially reduce the side-effects from the AgNPs application during theranostics cancer treatment.

The biologically active compounds produced by algae include lipids, sugars, proteins, antioxidants, vitamins, fats, sterols, enzymes, phenolics, terpenoids, flavonoids and other high value compounds of pharmaceutical and nutritional importance [19, 20, 66]. The major metabolites can be tentatively identified on the basis of their accurate mass and product positive and negative ions spectrum such as fatty acids, sterol lipids, pigment, N-acyl- α amino acids and their derivatives, benzonic acid ester.

Table 5. Metabolites identification from MCEs-CHL, HEX, MET and ETH by using LC-ESI-MS negative ionization mode [M-H(-)] (The symbol "+" indicates "Present", and "ND "indicates "Not detected").

Compounds			CHL			HEX			MET			ETH		
	t_R	m/z	*N. oculata*	*T. suecica*	*Chlorella sp.*	*N. oculata*	*T. suecica*	*Chlorella sp.*	*N. oculata*	*T. suecica*	*Chlorella sp.*	*N. oculata*	*T. suecica*	*Chlorella sp.*
1. Fatty acid														
Arachidoyl dodecanoate	29.26	479.48	+	ND	ND	+	ND	+	ND	ND	ND	ND	ND	ND
(+)-24-methyl-hexacosanoic acid	18.29	410.40	+	ND	ND	+	ND	+	ND	ND	ND	ND	ND	ND
Stearidonoyl-CoA	1.39	544.94	ND	ND	ND	ND	ND	ND	ND	+	+	ND	ND	+
Octadecanoic acid trichloroethyl ester	28.58	414.18	+	+	+	+	+	+	ND	ND	ND	ND	ND	ND
Octadecanoic acid trichloroethyl ester isomer	32.08	414.18	ND	+	+	+	+	+	+	+	+	+	+	+
2. Sterol lipids														
4 α-hydroxymethyl-5 α-Cholesta-8,24-dien-3β-ol	26.75	414.66	+	+	+	+	+	+	ND	ND	ND	ND	ND	ND
4,4-dimethyl-5 α-cholest-7-en-3β-ol	31.46	413.37	ND	ND	ND	+	+	+	ND	ND	ND	ND	ND	ND
Lanosterol	29.40	425.38	+	+	ND	+	+	+	ND	ND	+	+	ND	ND
Fucosterol	2.11	412.65	ND	ND	ND	ND	ND	ND	ND	ND	ND	+	+	ND
Campestanol	20.62	402.38	ND	ND	+	ND	+	+	ND	ND	ND	ND	ND	ND
Campestanol isomer	20.93	402.38	ND	ND	+	ND	+	+	ND	ND	ND	ND	ND	ND
3. Glycerolipid														
PE (6:0/6:0)	10.11	411.19	+	+	+	+	+	+	ND	ND	ND	ND	ND	ND
PA (P-20:0/17:2(9Z,12Z))	12.89	698.52	ND	ND	ND	ND	ND	ND	+	+	+	+	+	+
TG (12:0/12:0/14:1(9Z)) [iso3]	17.03	664.56	+	ND	ND	+	ND	ND	+	+	+	+	+	+
PE (14:0/16:1(9Z))	11.32	661.47	ND	ND	ND	ND	ND	ND	+	+	+	+	ND	+
DG (18:1(9Z)/18:2(9Z,12Z)/0:0)[iso2]	17.84	618.52	+	ND	ND	ND	ND	+	ND	ND	ND	ND	ND	ND
4. Triterpenoids														
4 α-formyl-4β-methyl-5 α-Cholesta-8,24-dien-3β-ol	31.76	425.34	ND	ND	ND	+	+	+	ND	ND	ND	ND	ND	ND
Obtusifoliol	28.64	425.38	+	+	ND	+	+	+	ND	ND	ND	ND	ND	ND
Squalene	27.73	410.39	+	+	ND	+	ND	ND	ND	ND	ND	ND	ND	ND
5. Carotenoids														
Apo-4′-lycopenoate	23.86	461.32	+	+	+	+	+	+	ND	ND	ND	+	+	+
Apo-8′-lycopenal	26.72	416.30	+	+	+	+	+	+	ND	ND	ND	ND	ND	ND
All-trans-β-carotene	1.4	536.87	ND	ND	+	ND	+	ND	ND	+	+	ND	+	ND
15,15′-dihydroxy-β-carotene	27.82	569.44	+	+	+	+	+	+	+	+	+	+	+	+
15,15′-dihydroxy-β-carotene isomer	28.66	569.44	+	+	+	+	+	+	+	+	+	+	+	+
β-carotene 15,15′ epoxide	31.63	552.88	ND	ND	+	+	ND	+	ND	ND	+	ND	ND	+
Neoxanthin	16.59	600.88	ND	ND	ND	ND	+	ND	ND	ND	ND	ND	ND	ND
6. Chlorophyll														
Protoporphyrin IX	11.22	561.25	ND	ND	ND	ND	ND	ND	ND	ND	ND	+	+	+
Protoporphyrin IX isomer	18.44	561.25	ND	ND	ND	ND	ND	ND	+	+	+	ND	ND	+
Coproporphyrinogen I	15.8	659.31	+	ND	+	ND	ND	ND	ND	ND	ND	+	ND	ND
Coproporphyrinogen I isomer	24.8	659.31	+	ND	+	ND	ND	ND	ND	ND	ND	+	+	+
7. Fatty amides														
N-palmitoyl phenylalanine	11.08	403.31	+	+	+	ND	ND	ND	ND	ND	ND	ND	ND	ND
N-palmitoyl phenylalanine isomer	15.81	403.31	+	+	+	ND	ND	ND	ND	ND	ND	ND	ND	ND
All trans-retinyl palmitate	23.38	523.45	+	ND	ND	+	ND	ND	ND	ND	+	+	ND	ND
All trans-retinyl palmitate isomer	24.66	523.45	ND	+	ND	+	ND	ND	ND	ND	ND	ND	ND	ND
N-oleoyl glutamine	13.68	410.31	+	+	+	+	+	+	+	+	+	+	+	+

(*continued on next page*)

Table 5 (*continued*)

Compounds			CHL			HEX			MET			ETH		
	t_R	*m/z*	*N. oculata*	*T. suecica*	*Chlorella sp.*	*N. oculata*	*T. suecica*	*Chlorella sp.*	*N. oculata*	*T. suecica*	*Chlorella sp.*	*N. oculata*	*T. suecica*	*Chlorella sp.*
N-oleoyl glutamine isomer	27.76	410.31	+	+	+	+	ND	ND	ND	ND	ND	ND	ND	ND
8. Amino acid														
Geranylgeranylcysteine	1.64	407.24	+	+	+	+	+	+	+	+	+	+	+	+
Geranylgeranylcysteine isomer	1.92	407.24	+	+	+	ND	+	ND	+	+	+	+	+	+
9. Vitamins														
Phylloquinone	1.59	450.77	+	+	+	+	+	ND	ND	ND	ND	ND	ND	+
Thiamin triphosphate	14.45	504.25	+	+	+	ND	ND	ND	ND	ND	ND	ND	ND	ND
Ascorbyl Palmitate	32.24	414.26	+	+	+	+	+	+	ND	ND	ND	ND	ND	ND
Ascorbyl Palmitate isomer	33.13	414.26	+	+	+	+	+	+	ND	ND	ND	ND	ND	ND
10. Others														
Gancaonin Q	15.11	406.17	+	ND	ND	ND	+	+	ND	ND	ND	ND	ND	+
Gancaonin Q isomer	15.32	406.17	ND	ND	+	+	+	+	ND	+	ND	+	+	+
Paratocarpin E	15.27	408.21	+	+	+	ND	ND	ND	ND	ND	ND	ND	ND	ND
2-methoxy-6-(all-trans-heptaprenyl) phenol	25.78	599.48	+	+	+	ND	ND	ND	+	+	+	+	+	+
2-methoxy-6 (all-trans-heptaprenyl) phenol isomer	26.61	599.48	+	+	+	ND	ND	ND	+	ND	+	+	ND	+
UDP- α-D-glucose	23.12	566.30	ND	ND	ND	ND	ND	ND	ND	+	+	+	ND	+
D-glucosyl-sphingosine	18.48	461.65	+	+	+	ND	ND	ND	ND	ND	ND	ND	ND	ND
D-glucosyl-sphingosine isomer	20.71	461.65	+	ND	ND	ND	ND	ND	ND	ND	ND	ND	ND	ND
8-oxo-dGDP	10.76	443.21	+	+	+	ND	ND	ND	+	ND	+	+	+	+
8-oxo-dADP	10.98	424.18	+	+	+	ND	ND	ND	+	+	+	+	+	+
2-(α-hydroxyethyl) thiamine diphosphate	10.43	468.06	+	+	+	ND	ND	ND	ND	ND	ND	ND	ND	ND
2-(α-hydroxyethyl) thiamine diphosphate isomer	26.81	468.06	+	ND	ND	ND	ND	ND	ND	ND	ND	ND	ND	ND
Geranylgeranyl diphosphate	22.90	450.45	+	ND	+	+	+	+	ND	ND	+	+	ND	ND
Geranylgeranyl diphosphate isomer	32.93	450.45	+	+	+	+	ND	ND	+	ND	+	ND	ND	+
Didecyl phthalate	1.81	446.73	ND	ND	ND	ND	ND	ND	ND	ND	ND	ND	+	ND
Leukotriene-D4	17.31	496.66	ND	ND	ND	+	ND	ND	ND	ND	ND	+	+	ND
Leukotriene-C4	19.94	625.30	ND	+	ND	ND	ND	ND	+	+	+	+	+	+
Leukotriene-C4 isomer	20.41	625.30	ND	ND	+	ND	ND	ND	+	+	+	+	+	+
Hexatriacontane	32.68	506.98	ND	ND	ND	ND	ND	ND	ND	+	ND	ND	ND	ND
Hexatriacontane isomer	33.14	506.98	ND	ND	ND	ND	ND	ND	ND	+	ND	+	ND	ND
Heptasiloxane, hexadecamethyl-	12.05	533.07	+	ND	+	ND	ND	ND	+	+	+	+	+	ND
Unknown	15.37	435.27	+	+	+	+	+	+	+	+	+	+	+	+

As the most comprehensive and largest libraries currently available contain only a small part of the endogenous metabolites found in the biological samples, the number of unidentified metabolites may be three times greater than the number of specific metabolites, even after comprehensive data processing [67]. For the negative ion mode in our study, the MCEs-W exhibited the presence of fatty acids stearidonoyl-CoA and octadecanoic acid trichloroethyl ester isomer. However, while the MCEs-ETH exhibited octadecanoic acid trichloroethyl ester isomer, only *Chlorella*-ETH showed stearidonoyl-CoA. For carotenoids and chlorophyll, the MCEs-ETH detected apo-4′-lycopenoate, 15,15′-dihydroxy-β-carotene and 15,15′-dihydroxy-β-carotene isomer, and the chlorophyll transformation products including protoporphyrin IX and coproporphyrinogen I isomer. Coproporphyrinogen I was detected in *N. oculata*- ETH; apo-8′-lycopenal and all-trans-β-carotene in *T. suecica*-ETH; and β-carotene 15,15′ epoxide and protoporphyrin IX isomer in *Chlorella* sp.-ETH. For the positive ion mode, the MCEs-W showed meso-Zeaxanthin/(3R, 3′S)-Zeaxanthin isomer, and protoporphyrinogen IX isomer. Methyl pyropheophorbide was also detected only in the MCEs-W. Other pigments detected were meso-Zeaxanthin/(3R,3′S)-Zeaxanthin; protoporphyrinogen IX in *N. oculata*-W and *T. suecica*-W. The MCEs-ETH showed the detection of fucoxanthin, all-trans-β-carotene, lutein and lutein isomer, and the two protoporphyrin IX isomers; violaxanthin in *N. oculata*-ETH and *Chlorella* sp.-ETH; protoporphyrin IX in *N. oculata*-ETH and *T. suecica*-ETH; all-trans-β-carotene isomer and meso-zeaxanthin/(3R, 3′S)-zeaxanthin isomer in *T. suecica*-ETH and *Chlorella* sp.-ETH; meso--zeaxanthin/(3R,3′S)-zeaxanthin in *Chlorella* sp.-ETH; and 15,15′-dihydroxy-&β-carotene in *T. suecica*-ETH. Fucoxanthin, violaxanthin and their derivatives were the two interesting compounds detected that could be explored further as anticancer agents or for malignant tumor inhibition [47, 48].

Other species such as *N. gaditana* has been characterized by the high lipids, around 65 and 70% (dry basis) [68], and the carotenoids such as

Table 6. Metabolites identification from MCEs-CHL, HEX, MET and ETH by using LC-ESI-MS of positive ionization mode [M + H(+)] (The symbol "+" indicates "Present", and "ND "indicates "Not detected").

Compounds			CHL			HEX			MET			ETH		
	t_R	m/z	*N. oculata*	*T. suecica*	*Chlorella sp.*	*N. oculata*	*T. suecica*	*Chlorella* sp.	*N. oculata*	*T. suecica*	*Chlorella sp.*	*N. oculata*	*T. suecica*	*Chlorella* sp.
1. Fatty acid														
22:6 Cholesteryl ester	31.54	696.59	ND	ND	ND	+	ND	ND	ND	ND	ND	ND	ND	ND
22:6 Cholesteryl ester isomer	32.83	696.59	+	ND	ND	+	+	+	ND	+	+	+	+	ND
1-palmitoylglycerol 3-phosphate	31.50	411.25	+	+	ND	ND	ND	ND	+	+	+	+	+	+
2. Sterol lipids														
Stoloniferone A	23.79	426.32	+	+	+	ND	ND	ND	+	+	+	+	+	+
4 α-carboxy-5 α-cholesta-8,24-dien-3β-ol	13.56	429.34	ND	+	ND	+	ND	ND	ND	ND	ND	ND	ND	ND
3. Triterpenoids														
4 α-formyl-5 α-cholesta-8,24-dien-3β-ol	20.45	413.34	ND	ND	+	+	ND	ND	ND	ND	ND	ND	ND	ND
4. Carotenoids														
Apo-4′-lycopenoate	29.60	499.36	ND	ND	+	+	ND	ND	ND	ND	ND	ND	ND	ND
Apo-4′-lycopenoate isomer	29.84	499.36	ND	ND	+	ND	ND	+	ND	+	+	ND	ND	ND
All-trans-β-carotene	1.46	536.89	+	+	+	+	+	+	ND	ND	ND	+	+	+
All-trans-β-carotene isomer	2.06	536.89	+	+	+	+	+	+	ND	ND	ND	ND	+	+
15,15′-dihydroxy-β-carotene	1.42	570.89	ND	ND	ND	ND	+	+	+	+	+	ND	+	ND
Meso-Zeaxanthin/ (3R,3′S)-Zeaxanthin	26.48	569.44	ND	ND	ND	ND	ND	ND	ND	ND	+	ND	ND	+
Meso-Zeaxanthin/ (3R,3′S)-Zeaxanthin isomer	32.91	569.44	+	+	ND	+	+	ND	+	+	ND	ND	+	+
α-Cryptoxanthin	14.55	553.41	+	ND	ND	ND	ND	ND	ND	ND	ND	ND	ND	ND
Violaxanthin	28.99	600.42	ND	ND	ND	ND	ND	ND	+	+	+	+	ND	+
Fucoxanthin	1.63	658.90	+	+	+	ND	ND	ND	ND	ND	ND	+	+	+
Lutein	1.44	568.87	ND	ND	ND	ND	+	ND	+	+	+	+	+	+
Lutein isomer	1.89	568.87	+	+	+	+	+	+	+	+	+	+	+	+
Neoxanthin	1.67	600.89	ND	ND	+	+	ND	ND	ND	ND	ND	ND	ND	ND
5. Chlorophyll														
Protoporphyrin IX	14.14	563.26	ND	ND	ND	ND	ND	ND	+	+	+	+	+	ND
Protoporphyrin IX isomer	16.37	563.26	ND	ND	ND	ND	ND	ND	+	+	+	+	+	+
Protoporphyrin IX isomer	17.52	536.26	ND	ND	ND	ND	ND	ND	ND	ND	ND	+	+	+
Protoporphyrinogen IX	20.03	591.29	ND	+	ND	ND	ND	ND	ND	ND	ND	ND	ND	ND
6. Fatty amides														
Termitomycamide B	16.11	436.30	ND	ND	ND	ND	ND	ND	ND	+	ND	ND	+	ND
Termitomycamide B isomer	20.60	436.30	ND	ND	ND	ND	ND	ND	+	+	ND	ND	+	+
Termitomycamide B isomer	29.00	436.30	ND	ND	+	ND	+	+	+	+	+	+	+	+
7. Amino acid														
N-arachidonoyl glutamic acid														
	14.76	433.28	ND	ND	ND	ND	ND	ND	ND	+	+	ND	+	ND
8. Vitamins														
Riboflavin cyclc-4′,5′-phosphate	18.20	438.32	ND	ND	ND	ND	ND	ND	ND	+	ND	ND	ND	+
β-Tocopherol isomer	12.71	416.37	ND	ND	ND	ND	+	ND	ND	ND	ND	ND	ND	ND
β-Tocopherol isomer	13.73	416.37	ND	ND	ND	ND	ND	ND	+	+	+	+	+	+
Ascorbyl Palmitate	13.58	415.26	ND	ND	ND	+	ND	ND	ND	ND	ND	ND	ND	ND
9. Others														
Quercetin 3-(2″-galloylrhamnoside)	17.25	600.11	ND	ND	ND	ND	ND	ND	ND	ND	+	ND	ND	ND
Quercetin 3-(2″-galloylrhamnoside) isomer	26.83	600.11	+	ND	ND	ND	ND	ND	ND	ND	ND	ND	ND	ND

(*continued on next page*)

Table 6 (*continued*)

Compounds			CHL			HEX			MET			ETH		
	t_R	*m/z*	*N. oculata*	*T. suecica*	*Chlorella sp.*	*N. oculata*	*T. suecica*	*Chlorella* sp.	*N. oculata*	*T. suecica*	*Chlorella sp.*	*N. oculata*	*T. suecica*	*Chlorella* sp.
Quercetin 7-methyl ether 3,3′,4′-trisulfate	20.95	555.93	ND	ND	ND	ND	ND	ND	ND	+	+	ND	+	ND
Erycristin	23.68	406.22	+	+	+	ND	ND	ND	+	ND	+	+	+	+
Kolaflavanone	14.67	588.23	ND	ND	ND	ND	ND	ND	ND	ND	+	+	+	ND
dTDP- α-D-glucose	12.15	564.33	ND	ND	ND	ND	ND	ND	+	ND	+	+	+	+
Cucurbitacin I 2-glucoside	9.77	676.37	ND	ND	ND	ND	ND	ND	+	+	+	+	+	+
dUDP	1.6	404.16	ND	ND	ND	ND	ND	ND	ND	ND	+	+	ND	ND
Phytanoyl-CoA	9.41	531.71	+	ND	+	ND	ND	ND	+	+	+	+	ND	+
Presqualene diphosphate	28.96	586.71	ND	ND	ND	ND	ND	ND	ND	ND	ND	ND	ND	+
Tetracontane	12.17	563.08	ND	ND	ND	ND	ND	ND	+	ND	+	+	ND	ND
Tetracontane isomer	19.59	563.08	ND	ND	ND	ND	ND	ND	ND	ND	+	ND	ND	ND
Tetracontane isomer	28.32	563.08	ND	ND	ND	ND	ND	+	ND	ND	ND	ND	ND	ND
Canthiumine	16.81	552.27	ND	ND	ND	ND	ND	ND	+	+	+	+	+	+
Heptasiloxane, hexadecamethyl-	15.91	533.14	ND	ND	ND	ND	ND	ND	ND	ND	ND	ND	+	+

β-carotene, astaxanthin, neoxanthin, canthaxanthin, zeaxanthin and violaxanthin [69]. Lutein, foloxanthin, zanthophils, neoxanthin, estrogen luroxanthin and anthraxanthin in *T. suecica* extracts have exhibited antioxidant activity and strong repair mechanism in the human lung cancer cell line (A549). The tissue repair effects are demonstrated in the reengineered human skin tissue cells "EpiDerm™" [70]. The most abundant antioxidants in the *Chlorella* extracts are the carotenoids, chlorophyll, chlorophyll *a* and *b*, phenophytes *a* and lutein [71]. The most abundant carotenoids include α and β-carotene, zeaxanthin, lutein, neoxanthin and phylaxanthin, while the ketocarotenoids like cantha-xanthin and astaxanthin are found in some *Chlorella* species [72]. Carotenoids in general exhibit anti-cancer, anti-obesity, anti-inflammatory, and anti-diabetic effects and have potential to cure heart disease [73]. Violaxanthin isolated from *C. ellipsoidea* has been proposed as a suitable candidate to tackle inflammatory disorders and identified as exhibiting anti-proliferative and pro-apoptotic effects against HCT116 human colon cancer cells [74]. Fucoxanthin and its metabolites, fucoxanthinol and halocynthiaxanthin, have shown anti-inflammatory, anti-mutagenic, anti-obesity, anti-neoplastic, anti-diabetic activity [48], and antioxidant activity with the decomposition of ROS such as $^{\bullet}OH$ and O^{2-} [75]. Fucoxanthin isomers including 13Z and 13′Z isomers also have high anti-proliferative activity in different cancer cell lines [49].

Several fatty amides, amino acids and vitamins were detected in the MCEs-W and ETH, to further promote the antioxidant activities of the MCEs in our study. The negative ion mode detected N-oleoyl glutamine and geranylgeranylcysteine in all MCEs; and geranylgeranylcysteine isomer in MCEs-W. The phylloquinone or vitamin K1 was identified in both MCEs-W and ETH; and all trans-retinyl palmitate was observed in *N. oculata*-ETH. For positive ion mode, phylloquinone was detected only in MCEs-W; ascorbyl stearate and ascorbyl stearate isomer only in *N. oculata*-W and *T. suecica*-W; riboflavin cyclic-4′,5′-phosphate in *N. oculata*-W; and β-tocopherol in *Chlorella* sp.-W. The amides including termitomycamide B isomer was found in MCEs-ETH; termitomycamide B isomer in *T. suecica*-ETH and *Chlorella* sp.-ETH; and termitomycamide B and N-arachidonoyl glutamic acid in *T. suecica*-ETH. The vitamin β-tocopherol isomer was detected in MCEs-ETH and riboflavin cyclic-4′,5′-phosphate in *Chlorella* sp.-ETH.

In our study, presqualene diphosphate, an intermediate in the biosynthesis of terpenoid [53], is found in *Chlorella* sp.-ETH. Squalene was detected in *N. oculata*-CHL and HEX and *T. suecica*-CHL, but none in the MCEs-W and ETH. Squalene, a triterpene and a precursor for the synthesis of cholesterol and steroid hormones in human body, does not induce scavenging activity or significantly affect the cell proliferation rates, cell cycle profile or apoptosis in human epithelial cells MCF10A and breast cancer cells (MDA-MB-231 and MCF-7) [76]. However, squalene in a dose-dependent manner, affects intracellular ROS level reduction, prevents oxidative injury from H_2O_2 and protects against DNA damage in epithelial MCF10A cells. Interestingly no similar effects of squalene are observed in the MCF7 and MDA-MB-231 cancer cells. Squalene, found in large quantities in virgin olive oils, has been suggested to be partially responsible for the low incidence of breast cancer in mediterranean diet groups. Other compound such as prenylated chalcone (Paratocarpin E) which has significant anti-cancer effects [51], is identified in *N. oculata*-W and *T. suecica*-W. Two phenols, 2-methoxy-6-(all-trans-heptaprenyl) phenol and 2-methoxy-6-(all-trans-heptaprenyl) phenol isomer, were observed in MCEs-ETH. Geranylgeranyl diphosphate (GGPP), one of the key isoprenoids for conversion into plant growth compounds, was found in *N. oculata*-W, *N. oculata*-ETH and *T. suecica*-W, and GGPP isomer was detected in *Chlorella* sp.-ETH. Didecyl phthalate, the benzoic acid esters derived from the oxidation of fatty acids in marine organisms, was found in the MCEs-W and *T. suecica*-ETH. Canthiumine, a cyclic peptide, was detected in the MCEs-ETH. Pyrimidine 2′-deoxyribonucleoside diphosphates, identified as dUDP, was detected in *N. oculata*-ETH; and phytanoyl CoA, a coenzyme A for the side chain of the chlorophyll [53], in *N. oculata*-ETH and *Chlorella* sp.-ETH.

The flavonoid quercetin 7-methyl ether 3,3′,4′-trisulfate was detected in *T. suecica*-ETH; erycristin in MCEs-ETH and kolaflavanone in *N. oculata* and *T. suecica*-ETH. Several flavonoid-like compounds such as gancaonin Q, 6-prenylapigenin, 6,8-diprenyleriodictyol, and 4-hydroxylon-chocarpin isolated from *Dorstenia genus*, exhibit anti-proliferative activities against leukemia and solid cancer cells, as well as AML12 normal hepatocytes, by arresting the cell cycle, inducing apoptosis through Caspase 3/7, and anti-angiogenic activities [77]. Amino acid profile of *Chlorella pyrenoidosa* includes phenylalanine, lysine, valine, threonine, methionine, histidine, leucine, isoleucine, and tryptophan. The contents of glutamine, asparagus and lysine have been reduced in *Chlorella* species and the total content of amino acids also decrease, a result of changes in the protein content [78]. The amino acids derived from oxaloacetate such as aspartate, lysine, asparagine, isoleucine, and threonine have also shown changes under temperature treatments [79]. The high anticancer activities of AgNPs-MCEs co-application against breast cancer in our study, suggests the ability of the AgNPs to interact with the metabolites in the MCEs to confer selective cytotoxicity on the breast cancer cells, but not on the non-cancerous Vero cells. The AgNPs may act as an adjuvant to the MCEs, and the antioxidative compounds, principally the carotenoids, may lessen the toxicity on the Vero cells [7]. The lower number of metabolites in the

MCEs-W did not affect the efficacy with the AgNPs, suggesting that key metabolites are important and enough to retain the cytotoxicity on MCF-7 and 4T1 cells, without affecting the Vero cells.

Other studies have reported the use of metal and non-metal based co-delivery of drugs. The AgNPs-based co-delivery of oseltamivir (Ag@OTV) has reportedly inhibited the H1N1 influenza virus activity through the ROS-mediated signaling pathways and, AKT and p53 phosphorylation activation [80]. The selenium-based nanoparticle for drug delivery has also been successful in inhibiting the virus activity. The surface functionalization of selenium NPs by amantadine (Se@AM) is designed to reflect the drug resistance induced by the influenza virus infection. The Se@AM which exhibits reduced toxicity, significantly prevents the ability of H1N1 influenza to infect the host cells by the inhibition of neuraminidase activity [81]. The surface of SeNPs loaded with aridiol (Se@ARB) with lower toxicity has obviously prevented the H1N1 virus infection. The Se@ARB interferes with the reaction between the H1N1 influenza virus and the host cells by inhibiting hemagglutinin (HA) and neuraminidase (NA) activity. Se@ARB can block H1N1 from infecting MDCK cells and prevent DNA fragmentation, chromatin condensation, and impede the ROS generation. The *in vivo* study further suggests that the Se@ARB could inhibit the lung infection in H1N1-infected mice [82]. Our study may have great implications in the theranostic application of the AgNPs for effective diagnosis and therapeutics during cancer treatment. The potential applications and the side-effects with the AgNPs treatments remain the major challenges to be resolved before it can be considered safe.

5. Conclusions

The AgNPs-MCEs–W, ETH at the 4:1 and 5:1 ratios showed much lower or no cytotoxic effects on the Vero cells whilst retaining the cytotoxicity on the MCF-7 and 4T1 cells, comparable to or better than the AgNPs-MCEs-CHL. There were low apoptotic events observed in Vero cells with the AgNPs-MCEs co-application, but dose dependent effects were exhibited in the MCF-7 and 4T1 cell lines with increased early and late apoptosis, cell cycle arrest in all phases and apoptotic events in sub G1 phase. The induction of apoptosis in the breast cancer cells was confirmed with enhanced the level of ADP/ATP ratios and Caspase 3/7 activities after 24 and 48 h treatments. Not all metabolites had the same LC-MS ionization mode, as some were detected only with either the negative or positive mode. Others such as apo-4′-lycopenoate, all-trans-β-carotene, 15,15′-dihydroxy-β-carotene, protoporphyrin IX, ascorbyl palmitate and heptasiloxane and hexadecamethyl, can be detected in both modes based on the polarity and chemical properties. Some of the metabolites were detected in all species and all extracts, while others were detected only in one species or extract. Less number of metabolites was detected in the W extracts such as stachyose, methyl pyrophaeophoribide, ascorbyl stearate and ascorbyl stearate isomer. Fucosterol, protoporphyrin IX, didecyl phthalate, presqualene diphosphate and heptasiloxane, hexadecamethyl were detected only in ETH extracts. However, the presence of MCEs-W and ETH with elevated AgNPs level showed reduced toxicity against the non-cancerous cells whilst retaining the potent anticancer activities against breast cancer cells. This finding may be of great interest for the theranostic applications during cancer treatment.

Declarations

Author contribution statement

H. Hussein: Conceived and designed the experiments; Performed the experiments; Analyzed and interpreted the data; Contributed reagents, materials, analysis tools or data; Wrote the paper.

M. Maulidiani: Analyzed and interpreted the data.

M. Abdullah: Conceived and designed the experiments; Analyzed and interpreted the data; Contributed reagents, materials, analysis tools or data; Wrote the paper.

Funding statement

This work was supported by the Fundamental Research Grant Scheme, Ministry of Higher Education, Malaysia (FRGS/1/2015/SG05/UMT/02/4).

Competing interest statement

The authors declare no conflict of interest.

Additional information

No additional information is available for this paper.

Acknowledgements

The authors thank the Science Officers in the Institute of Marine Biotechnology, Universiti Malaysia Terengganu, and for their assistance with the facilities for the experiments. Also to Mr. Syed Ahmad Tajudin and Mr. Haziq Hamid from the Laboratory of Animal Cell Culture in Universiti Sultan Zainal Abidin, Tembila Campus, Besut, Terengganu, for their assistance in the flow cytometric analyses.

References

[1] H. Ajab, J.O. Dennis, M.A. Abdullah, Synthesis and characterization of cellulose and hydroxyapatite-carbon electrode composite for trace plumbum ions detection and its validation in blood serum, Int. J. Biol. Macromol. 113 (2018) 376–385.
[2] H. Ajab, A.A.A. Khan, M.S. Nazir, A. Yaqub, M.A. Abdullah, Cellulose-hydroxyapatite carbon electrode composite for trace plumbum ions detection in aqueous and palm oil mill effluent: interference, optimization and validation studies, Environ. Res. 176 (2019) 108563.
[3] P.B. Tchounwou, C.G. Yedjou, A.K. Patlolla, D.J. Sutton, Heavy metals toxicity and the environment, Mol. Clin. Environ. Toxicol. 101 (2012) 133–164.
[4] L. Wang, Early diagnosis of breast cancer, Sensors 17 (2017) 1572.
[5] L. Dash, Biological Synthesis and Characterization of Silver Nanoparticles Using *Bacillus Thuringiensis*, M. SC. Diss. National Institute of Technology, 2013.
[6] X. Zhang, Z.G. Liu, W. Shen, S. Gurunathan, Silver nanoparticles: synthesis, characterization, properties, applications, and therapeutic approaches, Int. J. Mol. Sci. 17 (2016) 1534.
[7] H.A. Hussein, H. Mohamad, M.M. Ghazaly, A.A. Laith, M.A. Abdullah, Cytotoxic effects of *Tetraselmis suecica* chloroform extracts with silver nanoparticle co-application on MCF-7, 4 T1, and Vero cell lines, J. Appl. Phycol. 32 (2020) 127–143.
[8] H.A. Hussein, H. Mohamad, M.M. Ghazaly, A.A. Laith, M.A. Abdullah, Anticancer and antioxidant activities of *Nannochloropsis oculata* and *Chlorella* sp. extracts in co-applications with silver nanoparticle, J. King Saud. Univ. Sci. (2020) (JKSUS-D-20-00531R4 - Accepted).
[9] A. Majdalawieh, M.C. Kanan, O. El-kadri, S.M. Kanan, Recent advances in gold and silver nanoparticles: synthesis and applications, J. Nanosci. Nanotechnol. 14 (2014) 4757–4780.
[10] A. Wicki, D. Witzigmann, V. Balasubramanian, J. Huwyler, Nanomedicine in cancer therapy: challenges, opportunities, and clinical applications, J. Contr. Release 200 (2015) 138–157.
[11] S. Gurunathan, J.W. Han, A.A. Dayem, V. Eppakayala, J.H. Park, S.G. Cho, K.J. Lee, J.H. Kim, Green synthesis of anisotropic silver nanoparticles and its potential cytotoxicity in human breast cancer cells (MCF-7), J. Ind. Eng. Chem. 19 (2013) 1600–1605.
[12] T.F. Molinski, D.S. Dalisay, S.L. Lievens, J.P. Saludes, Drug development from marine natural products, Nat. Rev. Drug Discov. 8 (2009) 69–85.
[13] M.G. De Morais, B.D.S. Vaz, E.G. De Morais, J.A.V. Costa, Biologically active metabolites synthesized by microalgae, BioMed Res. Int. 2015 (2015).
[14] D.J. Newman, G.M. Cragg, Marine natural products and related compounds in clinical and advanced preclinical trials, J. Nat. Prod. 67 (2004) 1216–1238.
[15] M. Bhattacharjee, Pharmaceutically valuable bioactive compounds of algae, Asian J. Pharmaceut. Clin. Res. 9 (2016) 43.
[16] S. Bhagavathy, P. Sumathi, I.J.S. Bell, Green algae *Chlorococcum humicola*-a new source of bioactive compounds with antimicrobial activity, Asian Pac. J. Trop. Biomed. 1 (2011) S1–S7.
[17] E. Matich, LC-MS-based Metabolomics Analysis to Determine the Effect that Varying Growth Conditions Have on Microalgae, PhD. Diss. State University of New York at Buffalo, 2018.

[18] S. Sudjito, N. Hamidi, U. Yanuhar, I.N.G. Wardana, Potential and properties of marine microalgae *Nannochloropsis oculata* as biomass fuel feedstock, Int. J. Energy Env. Eng. 5 (2014) 279–290.

[19] M.A. Abdullah, S.M.U. Shah, S.M.M. Shanab, H.E.A. Ali, Integrated algal bioprocess engineering for enhanced productivity of lipid, carbohydrate and high-value bioactive compounds, Res. Rev. J. Microbiol. Biotechnol. 6 (2017) 61–92.

[20] M.A. Abdullah, A. Ahmad, S.M.U. Shah, S.M.M. Shanab, H.E.A. Ali, M.A.M. Abo-State, M.F. Othman, Integrated algal engineering for bioenergy generation, effluent remediation, and production of high-value bioactive compounds, Biotechnol. Bioproc. Eng. 21 (2016) 236–249.

[21] M.A. Abdullah, H.A. Hussein, Integrated algal biorefinery and palm oil milling for bioenergy, biomaterials and biopharmaceuticals, Int. Conf. Sust. Energy Green Tech. 463 (2020), 012084.

[22] W.S. Jo, K.M. Yang, H.S. Park, G.Y. Kim, B.H. Nam, M.H. Jeong, Y.J. Choi, Effect of microalgal extracts of *Tetraselmis suecica* against UVB-Induced photoaging in human skin fibroblasts, Toxicol. Res. 28 (2012) 241–248.

[23] S.M. Saad, Y.A.M. Yusof, W.Z.W. Ngah, Comparison between locally produced *Chlorella vulgaris* and *Chlorella vulgaris* from Japan on proliferation and apoptosis of liver cancer cell line, HepG2, *Malaysian*, J. Biochem. Mol. Biol. 13 (2006) 32–36.

[24] S.M.U. Shah, Cell Culture Optimization and Reactor Studies of green and Brown Microalgae for Enhanced Lipid Production, PhD. Diss. Universiti Teknologi PETRONAS, Seri Iskandar, Malaysia, 2014.

[25] A. Sombatsri, Y. Thummanant, T. Sribuhom, P. Wongphakham, T. Senawong, C. Yenjai, Atalantums H-K from the peels of *Atalantia monophylla* and their cytotoxicity, Nat. Prod. Res. (2019) 1–7.

[26] N.W. Sit, Y.S. Chan, S.C. Lai, L.N. Lim, G.T. Looi, P.L. Tay, Y.T. Tee, Y.Y. Woon, K.S. Khoo, H.C. Ong, *In vitro* antidermatophytic activity and cytotoxicity of extracts derived from medicinal plants and marine algae, J. Mycol. Med. 28 (2018) 561–567.

[27] S. Siddiqui, R. Ahmad, M.A. Khan, S. Upadhyay, I. Husain, A.N. Srivastava, Cytostatic and anti-tumor potential of ajwa date pulp against human hepatocellular carcinoma HepG2 cells, Sci. Rep. 9 (2019) 245.

[28] P. Fernández Freire, A. Peropadre, J.M.P. Martín, O. Herrero, M.J. Hazen, An integrated cellular model to evaluate cytotoxic effects in mammalian cell lines, Toxicol. Vitro 23 (2009) 1553–1558.

[29] M. Kumarihamy, D. Ferreira, E.M.C. Jr, R. Sahu, B.L. Tekwani, S.O. Duke, S. Khan, N. Techen, N.P.D. Nanayakkara, Antiplasmodial and cytotoxic cytochalasins from an endophytic fungus, Nemania sp. UM10M, isolated from a diseased Torreya taxifolia leaf, Molecules 24 (2019) 777.

[30] S. Mashjoor, M. Yousefzadi, M.A. Esmaeili, R. Rafie, Cytotoxicity and antimicrobial activity of marine macro algae (Dictyotaceae and Ulvaceae) from the Persian Gulf, Cytotechnology 68 (2015) 1717–1726.

[31] M. Mimeault, N. Jouy, P. Depreux, J.-P. Hénichart, Synergistic antiproliferative and apoptotic effects induced by mixed epidermal growth factor receptor inhibitor ZD1839 and nitric oxide donor in human prostatic cancer cell lines, Prostate 62 (2005) 187–199.

[32] E. Szliszka, Z.P. Czuba, K. Jernas, W. Król, Dietary flavonoids sensitize HeLa cells to tumor necrosis factor-related apoptosis-inducing ligand (TRAIL), Int. J. Mol. Sci. 9 (2008) 56–64.

[33] Sigma Aldrich, Fundamental Techniques in Cell Culture: a Laboratory Handbook, 2003.

[34] J.A.N. Desmyter, J.L. Melnick, W.E. Rawls, Defectiveness of interferon production and of rubella virus interference in a line of afri-can green monkey kidney cells (Vero), J. Virol. 2 (1968) 955–961.

[35] M. Prabaharan, J.J. Grailer, S. Pilla, D.A. Steeber, S. Gong, Folate-conjugated amphiphilic hyperbranched block copolymers based on Boltorn® H40, poly (l-lactide) and poly (ethylene glycol) for tumor-targeted drug delivery, Biomaterials 30 (2009) 3009–3019.

[36] S. Janitabar-Darzi, R. Rezaei, K. Yavari, *In vitro* cytotoxicity effects of (197)Au/PAMAMG4 and (198)Au/PAMAMG4 nanocomposites against MCF7 and 4T1 breast cancer cell lines, Adv. Pharmaceut. Bull. 7 (2017) 87–95.

[37] T. Mosmann, Rapid colorimetric assay for cellular growth and survival: application to proliferation and cytotoxicity assays, J. Immunol. Methods 65 (1983) 55–63.

[38] S. Sarojini, P. Senthilkumaar, V. Ramesh, Impact of ethanolic extract of *Mikania glomerata* on human breast cancer (MCF 7) cell line, Int. J. Adv. Sci. Res. 2 (2016) 94–193.

[39] M. Brentnall, L. Rodriguez-Menocal, R.L. De Guevara, E. Cepero, L.H. Boise, Caspase-9, caspase-3 and caspase-7 have distinct roles during intrinsic apoptosis, BMC Cell Biol. 14 (2013) 32.

[40] D.W. Nicholson, A. Ali, N.A. Thornberry, J.P. Vaillancourt, C.K. Ding, M. Gallant, Y. Gareau, P.R. Griffin, M. Labelle, Y.A. Lazebnik, N.A. Munday, S.M. Raju, M.E. Smulson, T.T. Yamin, V.L. Yu, D.K. Miller, Identification and inhibition of the ICE/CED-3 protease necessary for mammalian apoptosis, Nature 376 (1995) 37–43.

[41] M.P. Suffness, J. Pezzuto, Assays related to cancer drug discovery, in: Methods in Plant Biochemistry: Assays for Bioactivity, 1990, pp. 71–133.

[42] T. Srisawat, P. Chumkaew, W. Heed-Chim, Y. Sukpondma, K. Kanokwiroon, Phytochemical screening and cytotoxicity of crude extracts of vatica diospyroides *Symington* type LS, Trop. J. Pharmaceut. Res. 12 (2013) 71–76.

[43] R. Sathasivam, R. Radhakrishnan, A. Hashem, E.F. Abd_Allah, Microalgae metabolites: a rich source for food and medicine, Saudi J. Biol. Sci. 26 (2019) 709–722.

[44] C.M. Paton, J.M. Ntambi, Biochemical and physiological function of stearoyl-CoA desaturase, Am. J. Physiol. Metab. 297 (2009) E28–E37.

[45] P. Suttiarporn, W. Chumpolsri, S. Mahatheeranont, S. Luangkamin, S. Teepsawang, V. Leardkamolkarn, Structures of phytosterols and triterpenoids with potential anti-cancer cctivity in bran of black non-glutinous rice, Nutrients 7 (2015) 1672–1687.

[46] M. Fabris, M. Matthijs, S. Carbonelle, T. Moses, J. Pollier, R. Dasseville, G.J.E. Baart, W. Vyverman, A. Goossens, Tracking the sterol biosynthesis pathway of the diatom *Phaeodactylum tricornutum*, New Phytol. 204 (2014) 521–535.

[47] V. Pasquet, et al., Antiproliferative activity of violaxanthin isolated from bioguided fractionation of *Dunaliella tertiolecta* extracts, Mar. Drugs 9 (2011) 819–831.

[48] L.J. Martin, Fucoxanthin and its metabolite fucoxanthinol in cancer prevention and treatment, Mar. Drugs 13 (2015) 4784–4798.

[49] B. Gilbert-López, J.A. Mendiola, J. Fontecha, L.A.M. van den Broek, L. Sijtsma, A. Cifuentes, M. Herreroa, E. Ibáñez, Downstream processing of Isochrysis galbana: a step towards microalgal biorefinery, Green Chem. 17 (2015) 4599–4609.

[50] P.M. Dewick, Medicinal Natural Products: a Biosynthetic Approach, third ed., John Wiley & Sons, 2009.

[51] S. Gao, D. Sun, G. Wang, J. Zhang, Y. Jiang, G. Li, K. Zhang, L. Wang, J. Huang, L. Chen, Growth inhibitory effect of paratocarpin E, a prenylated chalcone isolated from *Euphorbia humifusa* Wild., by induction of autophagy and apoptosis in human breast cancer cells, Bioorg. Chem. 69 (2016) 121–128.

[52] M.S. Brown, J.L. Goldstein, Mad bet for Rab, Nature 366 (1993) 14.

[53] National Center for Biotechnology Information, PubChem Database, Phytanoyl-CoA, 2019. CID=439640, https://pubchem.ncbi.nlm.nih.gov/compound/Phytanoyl-CoA.

[54] P.H. Baudelet, A.L. Gagez, J.B. Bérard, C. Juin, N. Bridiau, R. Kaas, V. Thiéry, J.P. Cadoret, L. Picot, Antiproliferative activity of *Cyanophora paradoxa* pigments in melanoma, breast and lung cancer cells, Mar. Drugs 11 (2013) 4390–4406.

[55] P.Y. Lin, C.T. Tsai, W.L. Chuang, Y.H. Chao, I. H Pan, Y.K. Chen, C.C. Lin, B.Y. Wang, *Chlorella sorokiniana* induces mitochondrial-mediated apoptosis in human non-small cell lung cancer cells and inhibits xenograft tumor growth *in vivo*, BMC Compl. Alternative Med. 17 (2017) 88.

[56] S.M.M. Shanab, S.S.M. Mostafa, E.A. Shalaby, G.I. Mahmoud, Aqueous extracts of microalgae exhibit antioxidant and anticancer activities, Asian Pac. J. Trop. Biomed. 2 (2012) 608–615.

[57] C. Rejeeth, B. Nataraj, R. Vivek, M. Sakthivel, Biosynthesis of silver nanoscale particles using *Spirulina platensis* induce growth-inhibitory effect on human breast cancer cell line MCF-7, Med. Aromatic Plants 3 (2014) 1000163.

[58] S. Gurunathan, J.W. Han, D.N. Kwon, J.H. Kim, Enhanced antibacterial and anti-biofilm activities of silver nanoparticles against Gram-negative and Gram-positive bacteria, Nanoscale Res. Lett. 9 (2014) 373, 2014.

[59] A.M. Fayaz, K. Balaji, M. Girilal, R. Yadav, P.T. Kalaichelvan, R. Venketesan, Biogenic synthesis of silver nanoparticles and their synergistic effect with antibiotics: a study against gram-positive and gram-negative bacteria, Nanomed. Nanotechnol. Biol. Med. 6 (2010) 103–109.

[60] J.R. Morones-Ramirez, J.A. Winkler, C.S. Spina, J.J. Collins, Silver enhances antibiotic activity against gram-negative bacteria, Sci. Transl. Med. 5 (2013), 190ra81-190ra81.

[61] M. Rajoo, A. Parolia, A. Pau, F.D. Amalraj, The role of propolis in inflammation and orofacial pain: a review, Annu. Res. Rev. Biol. 4 (2014) 651–664.

[62] P. Chokhachi, A. Mohammadi, B. Mansoori, S. Chokhachi, B. Baradaran, Growth inhibitory effect of *Scrophularia oxysepala* extract on mouse mammary carcinoma 4T1 cells *in vitro* and *in vivo* systems, Biomed. Pharmacother. 85 (2017) 718–724.

[63] J. Dai, R.J. Mumper, Plant phenolics: extraction, analysis and their antioxidant and anticancer properties, Molecules 15 (2010) 7313–7352.

[64] Q.D. Do, A.E. Angkawijaya, P.L. Tran-Nguyen, L.H. Huynh, F.E. Soetaredjo, S. Ismadji, Y.H. Ju, Effect of extraction solvent on total phenol content, total flavonoid content, and antioxidant activity of *Limnophila aromatica*, J. Food Drug Anal. 22 (2014) 296–302.

[65] K.H.S. Farvin, A. Surendraraj, A. Al-Ghunaim, F. Al-Yamani, Chemical profile and antioxidant activities of 26 selected species of seaweeds from Kuwait coast, J. Appl. Phycol. 31 (2019) 2653–2668.

[66] I. Priyadarshani, B. Rath, Commercial and industrial applications of micro algae–A review, J. Algal. Biomass Utln. 3 (2012) 89–100.

[67] X. Du, S.H. Zeisel, Spectral deconvolution for gas chromatography mass spectrometry-based metabolomics: current status and future perspectives, Comput. Struct. Biotechnol. J. 4 (2013), e201301013.

[68] D. Simionato, E. Sforza, E.C. Carpinelli, A. Bertucco, G.M. Giacometti, T. Morosinotto, Acclimation of *Nannochloropsis gaditana* to different illumination regimes: effects on lipids accumulation, Bioresour. Technol. 102 (2011) 6026–6032.

[69] L.M. Lubián, O. Montero, I. Moreno-Garrido, I.E. Huertas, C. Sobrino, M. González-del Valle, G. Parés, *Nannochloropsis* (Eustigmatophyceae) as source of commercially valuable pigments, J. Appl. Phycol. 12 (2000) 249–255.

[70] C. Sansone, et al., The green microalga *Tetraselmis suecica* reduces oxidative stress and induces repairing mechanisms in human cells, Sci. Rep. 7 (2017) 41215.

[71] K.H. Cha, S.W. Kang, C.Y. Kim, B.H. Um, Y.R. Na, C.H. Pan, Effect of pressurized liquids on extraction of antioxidants from *Chlorella vulgaris*, J. Agric. Food Chem. 58 (2010) 4756–4761.

[72] Y. Aluç, G. Başaran Kankılıç, İ. Tüzün, Determination of carotenoids in two algae species from the saline water of *Kapulukaya reservoir* by HPLC, J. Liq. Chromatogr. Relat. Technol. 41 (2018) 93–100.

[73] V.H. Chuyen, J.B. Eun, Marine carotenoids: bioactivities and potential benefits to human health, Crit. Rev. Food Sci. Nutr. 57 (2017) 2600–2610.

[74] K.H. Cha, S.Y. Koo, D.U. Lee, Antiproliferative effects of carotenoids extracted from *Chlorella ellipsoidea* and *Chlorella vulgaris* on human colon cancer cells, J. Agric. Food Chem. 56 (2008) 10521–10526.

[75] N.M. Sachindra, E. Sato, H. Maeda, M. Hosokawa, Y. Niwano, M. Kohno, K. Miyashita, Radical scavenging and singlet oxygen quenching activity of marine carotenoid fucoxanthin and its metabolites, J. Agric. Food Chem. 55 (2007) 8516–8522.

[76] F. Warleta, M. Campos, Y. Allouche, C. Sánchez-Quesada, J. Ruiz-Mora, G. Beltrán, J.J. Gaforio, Squalene protects against oxidative DNA damage in MCF10A human mammary epithelial cells but not in MCF7 and MDA-MB-231 human breast cancer cells, Food Chem. Toxicol. 48 (2010) 1092–1100.

[77] V. Kuete, B. Ngameni, B. Wiench, B. Krusche, C. Horwedel, B.T. Ngadjui, T. Efferth, Cytotoxicity and mode of action of four naturally occuring flavonoids from the genus Dorstenia: gancaonin Q, 4-Hydroxylonchocarpin, 6-Prenylapigenin, and 6,8-Diprenyleriodictyol, Planta Med. 77 (2011), 1984–1989.

[78] H. Safafar, P. Uldall Nørregaard, A. Ljubic, P. Møller, S. Løvstad Holdt, C. Jacobsen, Enhancement of protein and pigment content in two *Chlorella* species cultivated on industrial process water, J. Mar. Sci. Eng. 4 (2016) 84.

[79] S.S. Gill, S. Willette, B. Dungan, J.M. Jarvis, T. Schaub, D.M. Vanleeuwen, R.S. Hilaire, F.O. Holguin, Suboptimal temperature acclimation affects kennedy pathway gene expression, lipidome and metabolite profile of *Nannochloropsis salina* during PUFA enriched TAG synthesis, Mar. Drugs 16 (2018) 425.

[80] Y. Li, Z. Lin, M. Zhao, T. Xu, B. Wang, L. Hua, H. Wang, H. Xia, B. Zhu, Silver nanoparticles based co-delivery of *Oseltamivir* to inhibit the activity of H1N1 influenza virus through ROS-mediated signaling pathways, ACS Appl. Mater. Interfaces 8 (2016) 24385–24393.

[81] Y. Li, Z. Lin, M. Guo, M. Zhao, Y. Xia, C. Wang, T. Xu, B. Zhu, Inhibition of H1N1 influenza virus-induced apoptosis by functionalized selenium nanoparticles with amantadine through ROS-mediated AKT signaling pathways, Int. J. Nanomed. 13 (2018) 2005–2016.

[82] Y. Li, Z. Lin, G. Gong, M. Guo, T. Xu, C. Wang, M. Zhao, Y. Xia, Y. Tang, J. Zhong, Y. Chen, L. Hua, Y. Huang, F. Zeng, B. Zhu, Inhibition of H1N1 influenza virus-induced apoptosis by selenium nanoparticles functionalized with arbidol through ROS-mediated signaling pathways, J. Mater. Chem. B 7 (2019) 4252–4262.

[83] H.A. Hussein, M.N.I. Kassim, M. Maulidiani, F. Abas, M.A. Abdullah, Cytotoxicity and ^{1}H NMR metabolomics analyses of microalgal extracts with Tamoxifen co-application on breast cancer cells without affecting Vero cells, Saudi J. Biol. Sci. (2020) (SJBS-D-20-00166 - Under review).